

Resolving Deep Phylogenetic Relationships in Salamanders: Analyses of Mitochondrial and Nuclear Genomic Data

DAVID W. WEISROCK,^{1,2} LUKE J. HARMON,¹ AND ALLAN LARSON¹

¹Department of Biology, Campus Box 1137, Washington University, St. Louis, Missouri 63130, USA

²Present Address: Department of Biology, University of Kentucky, Lexington, Kentucky 40506, USA; E-mail: weisrock@uky.edu

Abstract.—Phylogenetic relationships among salamander families illustrate analytical challenges inherent to inferring phylogenies in which terminal branches are temporally very long relative to internal branches. We present new mitochondrial DNA sequences, approximately 2100 base pairs from the genes encoding ND1, ND2, COI, and the intervening tRNA genes for 34 species representing all 10 salamander families, to examine these relationships. Parsimony analysis of these mtDNA sequences supports monophyly of all families except Proteidae, but yields a tree largely unresolved with respect to interfamilial relationships and the phylogenetic positions of the proteid genera *Necturus* and *Proteus*. In contrast, Bayesian and maximum-likelihood analyses of the mtDNA data produce a topology concordant with phylogenetic results from nuclear-encoded rRNA sequences, and they statistically reject monophyly of the internally fertilizing salamanders, suborder Salamandroidea. Phylogenetic simulations based on our mitochondrial DNA sequences reveal that Bayesian analyses outperform parsimony in reconstructing short branches located deep in the phylogenetic history of a taxon. However, phylogenetic conflicts between our results and a recent analysis of nuclear RAG-1 gene sequences suggest that statistical rejection of a monophyletic Salamandroidea by Bayesian analyses of our mitochondrial genomic data is probably erroneous. Bayesian and likelihood-based analyses may overestimate phylogenetic precision when estimating short branches located deep in a phylogeny from data showing substitutional saturation; an analysis of nucleotide substitutions indicates that these methods may be overly sensitive to a relatively small number of sites that show substitutions judged uncommon by the favored evolutionary model. [Bayesian; DNA simulation; internal fertilization; mitochondrial DNA; parsimony; ribosomal RNA; salamander.]

Phylogenetic relationships among taxonomic families of salamanders are difficult to resolve because branches grouping multiple families are likely very short relative to the subsequent evolutionary history of the group (Larson et al., 2003). Parsimony-based analyses of morphological characters and nuclear-encoded rRNA sequences produce different phylogenetic topologies with statistically significant conflict between these data sets (Larson and Dimmick, 1993; Larson, 1998). Analyses of an expanded set of morphological characters and sequences from the nuclear RAG-1 gene likewise show that resolution of deep phylogenetic relationships varies among data partitions and phylogenetic methods (Wiens et al., 2005).

Analyses of combined morphological and molecular data support monophyly of internally fertilizing salamanders, suborder Salamandroidea (families Ambystomatidae, Amphiidae, Dicamptodontidae, Plethodontidae, Proteidae, Rhyacotritonidae, and Salamandridae; Larson and Dimmick, 1993; Wiens et al., 2005), although this grouping is rejected statistically by two independent molecular data sets, the nuclear-encoded rRNA sequences and the mitochondrial genomic sequences reported here.

Nonmonophyly of Salamandroidea requires homoplastic evolution of internal fertilization, a complex syndrome of characters involving morphology of male and female cloacal glands, life history and behavior (see Sever and Brizzi, 1998) or secondary loss of this trait. Independent evolution of internal fertilization by multiple lineages seems unlikely (Sever and Brizzi, 1998). Absence of evolutionary loss of this syndrome within families indicates that it is indispensable to the species that have it and therefore highly “burdened” using the terminology of Riedl (1978) and Donoghue (1989); such characters

are unlikely to be secondarily lost. External fertilization, as observed in suborder Cryptobranchoidea (families Cryptobranchidae and Hynobiidae) and strongly inferred for suborder Sirenoidea (family Sirenidae; Sever et al., 1996), is considered ancestral for salamanders and anuran amphibians.

To reexamine these relationships and the phylogenetic-information content of molecular characters, we present new mitochondrial DNA (mtDNA) sequences, approximately 2100 base pairs from the genes encoding ND1, ND2, COI, and the intervening tRNA genes. Our phylogenetic analyses apply parsimony, maximum-likelihood, and Bayesian criteria (Huelsenbeck et al., 2001; Swofford et al., 1996) to test alternative phylogenetic hypotheses using both new mtDNA data and previously published morphological and nuclear rRNA data (Larson, 1991; Larson and Dimmick, 1993). We use a variety of statistical tests to evaluate alternative phylogenetic hypotheses derived from both a priori information (e.g., monophyly of suborder Salamandroidea) as well as a posteriori hypotheses generated from our new phylogenetic results. We identify and describe the molecular characters that make large contributions to statistically significant phylogenetic results obtained from maximum-likelihood and Bayesian methods.

Because the evolutionary age of salamanders is at least 150 My (Gao and Shubin, 2001) and fossil evidence dates some extant families to the upper Cretaceous (Gao and Shubin, 2003), branches grouping two or more families are probably short relative to their phylogenetic depth. Previous attempts at using mtDNA sequence (12S and 16S rRNA) data to resolve salamander-family phylogeny produced a tree with extremely long terminal branches and short, poorly supported interfamilial branches (Hay et al., 1995), indicating that family-level cladogenesis

occurred over a relatively short time interval. In such cases, misleading phylogenetic information generated by parallel substitutions among branches within taxonomic families may overwhelm the signal generated by substitutions on a lineage ancestral to two or more families. Phylogenetic signal is eroded further by multiple substitutions occurring at the sites containing the original phylogenetic signal. Phylogenetic reconstruction of such evolutionary histories can be misled by long-branch attraction (Felsenstein, 1978; Huelsenbeck, 1997; Swofford et al., 2001). In extreme cases, a bifurcating tree may be analytically indistinguishable from a polytomy (see discussion by Donoghue and Sanderson [1992], Fishbein et al. [2001], Jackman et al. [1999], Misof et al. [2001], Poe and Chubb [2004], Slowinski [2001], and Walsh et al. [1999]). We explore the limits of deep phylogenetic reconstruction in the evolutionary history of salamanders using simulations based on the inferred evolutionary models of our mtDNA sequences.

MATERIALS AND METHODS

Taxon Sampling

This study used the published morphological and nuclear rRNA sequence data matrices of Larson and Dimmick (1993). The morphological data used by Larson and Dimmick (1993) are compiled from other sources representing head and trunk morphology (Duellman and Trueb, 1986) and cloacal characters related to fertilization (Sever 1991a, 1991b; 1994). The complete data matrix containing all taxa and morphological characters from Larson and Dimmick (1993) was used in combined analyses with molecular characters.

Nuclear rRNA sequence data were taken from Larson and Dimmick (1993) and Larson (1991) and included the anuran outgroup *Xenopus laevis*, the caecilian out-group, *Typhlonectes compressicauda*, and 24 ingroup taxa representing all ten salamander families (Table 1). Ten ingroup samples from Larson (1991) were excluded from our analyses because they are identical or nearly identical to analyzed samples representing the same taxonomic family. This reduction in sampling made heuristic parsimony and likelihood searches and bootstrap resampling computationally manageable.

Taxon sampling for the mtDNA data closely matched that of the nuclear rRNA sequence data (Table 1). When possible, tissue samples from the same specimen were used for the nuclear rRNA and mtDNA data; in all other cases but one (Rhyacotritonidae), another specimen of the same species was used. The mtDNA data set contained samples of 38 taxa, including 4 outgroup and 34 ingroup taxa covering all 10 salamander families. This included mitochondrial sequence for *Proteus anguinus*, a European troglodytic salamander grouped with the North American genus *Necturus* in the family Proteidae. Placement of these genera within the same family is the most dubious of all salamander-family groupings. Sequences for two outgroup taxa, *Rana catesbeiana* and *Typhlonectes natans*, and three ingroup taxa, *Chioglossa*

lusitanica, *Notophthalmus viridescens*, and *Salamandra salamandra*, were taken from GenBank (Table 1).

Taxon sampling in combined phylogenetic analyses followed two approaches. Because not all data were available for all taxa across data sets, we assembled pruned data sets that minimized the amount of missing data. Wiens (2003) showed that accuracy of phylogenetic analyses of incomplete data may be high if each taxon sampled contains sufficient characters; therefore, we also assembled combined data sets using the full complement of taxa from the mtDNA data set with rRNA and morphological data missing for some taxa.

DNA Extraction and Sequencing

DNA extraction, polymerase chain reaction, and sequencing methods were as described by Weisrock et al. (2001) except that some sequencing reactions were performed using a Big-Dye Terminator Ready-Reaction Kit (Perkin-Elmer) and run on an ABI (PE Applied Biosystems, Inc.) 373A automated DNA sequencer. We sequenced approximately 2100 contiguous bases of mitochondrial DNA including the genes encoding ND1 (sub-unit one of NADH dehydrogenase), tRNA^{Ile}, tRNA^{Gln}, tRNA^{Met}, ND2 (subunit two of NADH dehydrogenase), tRNA^{Trp}, tRNA^{Ala}, tRNA^{Asn}, tRNA^{Cys}, tRNA^{Tyr}, and COI (subunit I of cytochrome *c* oxidase), plus the origin for light-strand replication (O_L) between the tRNA^{Asn} and tRNA^{Cys} genes. This block of sequence also contains a small number of bases of intergenic sequence separating some tRNA genes. Primers used for sequencing are listed in Table 2.

Sequence Alignments

Alignment of the nuclear rRNA sequence data was similar to the original alignments of Larson (1991) and of Larson and Dimmick (1993) except for some length-variable segments in divergent domains of rRNA where alignment was considered ambiguous. These regions were excluded from all analyses.

Alignment of the mtDNA sequences was performed manually using amino acid sequence translations for protein-coding genes and secondary-structural models for tRNA genes (Kumazawa and Nishida, 1993). Length-variable regions whose alignment was ambiguous, including tRNA loops, all intergenic sequence, and much of the origin for light-strand replication (O_L), were excluded from all phylogenetic analyses.

All new mtDNA sequences have been deposited in GenBank under accession numbers AY916014 to AY916045. Data alignments for the mtDNA and nuclear rRNA character matrices have been placed in TreeBase under accession number S1237.

Phylogenetic Analyses

Parsimony analysis was performed on the mtDNA and nuclear rRNA data using PAUP* v4.0 (Swofford, 2002). A heuristic search option with 100 random-addition replicates was used with equal weighting of

TABLE 1. Taxon sampling utilized for nuclear rRNA and mtDNA sequence data.

Outgroup/ Salamander family	Taxa sampled nuclear rRNA data set	Museum/ tissue no.	Taxa sampled mtDNA data set	Museum/ tissue no.	GenBank no.
Anuran	<i>Xenopus laevis</i>	No voucher ^a	<i>Rana catesbeiana</i> <i>Xenopus laevis</i>	—	AF314016 NC001573
Caecilian	<i>Typhlonectes compressicauda</i>	FC12006	<i>Typhlonectes compressicauda</i> <i>Typhlonectes natans</i>	FC11146	AY91604 AF154051
Ambystomatidae	<i>Ambystoma californiense</i> <i>Ambystoma maculatum</i> <i>Ambystoma tigrinum</i>	MVZ161802 MVZ187998	<i>Ambystoma californiense</i> <i>Ambystoma tigrinum</i>	MVZ161803 MVZ187202	AY91605 AY91606
Amphiumidae	<i>Amphiuma means</i> <i>Amphiuma tridactylum</i>	MVZ144879 No voucher	<i>Amphiuma means</i> <i>Amphiuma pholeter</i> <i>Amphiuma tridactylum</i>	MVZ144889 No voucher	AY916037 AY916035 AY916036
Cryptobranchidae	<i>Andrias davidianus</i> <i>Cryptobranchus alleganiensis</i>	MVZ204245 INHS11236	<i>Andrias davidianus</i> <i>Cryptobranchus alleganiensis</i>	MVZ204245 INHS11236	AY916038 AY916039
Dicamptodontidae	<i>Dicamptodon aterrimus</i>	MVZ208187	<i>Dicamptodon aterrimus</i> <i>Dicamptodon tenebrosus</i>	MVZ203271 MVZ187929	AY91607 AY91608
Hynobiidae	<i>Batrachuperus mustersi</i> <i>Hynobius leechii</i> <i>Hynobius nebulosus</i> <i>Onychodactylus japonicus</i> <i>Salamandrella keyserlingii</i>	MVZ232869 MVZ169094 DMG3466 No voucher ^b DMG3467	<i>Batrachuperus mustersi</i> <i>Hynobius leechii</i> <i>Hynobius nebulosus</i> <i>Onychodactylus fischeri</i> <i>Onychodactylus japonicus</i> <i>Salamandrella keyserlingii</i>	MVZ232869 MVZ163727 KUHE24698 MVZ163731 No voucher ^b MVZ 222330	AY916034 AY916029 AY916030 AY916033 AY916032 AY916031
Plethodontidae	<i>Desmognathus ochrophaeus</i> <i>Eurycea longicauda</i> <i>Pseudoeurycea rex</i> <i>Pseudotriton montanus</i>	MVZ137266 No voucher ^c FC12359 MVZ137300	<i>Desmognathus ochrophaeus</i> <i>Eurycea longicauda</i> <i>Parvimolge townsendi</i> <i>Pseudoeurycea rex</i> <i>Pseudotriton montanus</i> <i>Stereochilus marginatus</i>	MVZ137267 No voucher ^c S8674 FC12359 MVZ137300 FC10268	AY916020 AY916023 AY916024 AY916025 AY916021 AY916022
Proteidae	<i>Necturus beyeri</i>	FC13770	<i>Necturus alabamensis</i> <i>Necturus beyeri</i> <i>Necturus lewisi</i> <i>Proteus anguinus</i> ^d	MVZ187705 MVZ187709 FC13623 No voucher	AY916043 AY916044 AY916042 AY916045
Rhyacotritonidae	<i>Rhyacotriton kezleri</i>	MVZ197368	<i>Rhyacotriton variegatus</i>	MVZ222581	AY916019
Salamandridae	<i>Notophthalmus viridescens</i> <i>Pleurodeles waltl</i> <i>Taricha rivularis</i>	MVZ161843 MVZ162383 MVZ161862	<i>Chioglossa lusitanica</i> <i>Notophthalmus viridescens</i> <i>Pleurodeles waltl</i> <i>Salamandra salamandra</i> <i>Salamandrina terdigitata</i> <i>Taricha rivularis</i>	MVZ230958 MVZ230959 MVZ162384 MVZ186046 MVZ178849 MVZ158853	AF296620 AF296616 AY916026 AF296622 AY916022 AY916027
Sirenidae	<i>Siren intermedia</i> <i>Siren lacertina</i>	MVZ144878 MVZ161877	<i>Siren intermedia</i> <i>Siren lacertina</i>	MVZ144877 MVZ161877	AY916040 AY916041

DMG number: Tissues used from the Redpath Museum.

FC and S numbers: Tissues used from the Museum of Vertebrate Zoology for which an animal voucher was not available.

INHS number: Specimen vouchered in the collections of the Illinois Natural History Survey.

KUHE number: Specimen vouchered in the collections of the Kyoto University Graduate School of Human and Environmental Studies.

MVZ numbers: Tissues used from the Museum of Vertebrate Zoology which have an animal voucher available.

^aOriginally published in Salim and Maden (1981).

^bCollected 1/4 mile west of Nikko, Tochigi Prefecture, Japan.

^cCollected 5 mi. south of Murphysboro, Jackson Co., Illinois.

^dBlood sample provided by R. Highton.

all characters and TBR branch swapping. To assess support for branches in the parsimony trees, bootstrap analysis was applied using 1000 bootstrap replicates with 100 random additions per replicate, and decay indices (Bremer, 1994) were calculated for each internal branch using TreeRot, v2.0 (Sorenson, 1999) and PAUP* v4.0 (Swofford, 2002). To test alternative phylogenetic hypotheses using parsimony, we used the Wilcoxon signed-ranks (WS-R) test (Templeton, 1983) as implemented in PAUP* v4.0. A number of a priori phylogenetic hypotheses were tested based on current classification and results from previous phylogenetic studies. To test these hypotheses we used the most parsimonious topology

compatible with the alternative hypothesis for the data being examined. To generate these alternative topologies, a constraint tree was generated using MacClade v4.0 (Maddison and Maddison, 2000) and implemented in a parsimony search using PAUP* v4.0. All alternative topologies tested in this study are presented in Appendix 1 (available at www.systematicbiology.org).

Maximum-likelihood (ML) phylogenetic analysis was performed on the individual mtDNA and nuclear rRNA data sets using PAUP* v4.0 with a heuristic search option and stepwise addition of taxa, 10 random-addition replicates, and TBR branch swapping. Likelihood-ratio tests implemented in the program Modeltest v3.06 (Posada

TABLE 2. List of mtDNA primers. Primers are designated by their 3' ends corresponding to numbered positions in the human mitochondrial genome (Anderson et al., 1981). H and L denote primers whose extension produces the heavy and light strands, respectively. Positions with mixed bases are labeled with standard one-letter codes: R = G or A, Y = T or C, and N = any base.

Primer	Sequence	Reference
L3002	5' TACGACCTCGATGTTGGATCAGG 3'	(Macey et al., 1997a)
L3878	5' GCCCCATTGACCTCACAGAAGG 3'	(Macey et al., 1998b)
L3878a	5' GCCCCATTGAYCTCACAGARGG 3'	This Study
L3878b	5' CCCCCATTGAYCTAACTGARGG 3'	This Study
L3878c	5' AGCCCCTTGAYCTCACAGARGG 3'	This Study
H4141	5' AGTTGGTCRTAGCGGAANCG 3'	(Macey et al., 2001)
L4160	5' CGATTCCGATATGACCARCT 3'	(Kumazawa and Nishida, 1993)
L4178b	5' CAACTAATACACCTACTATGAAA 3'	(Macey et al., 1997a)
L4221	5' AAGGATTACTITGATAGAGT 3'	(Macey et al., 1997a)
L4419	5' GGTATGGGCCAAAGCTT 3'	(Macey et al., 1998b)
L4437	5' AAGCTTCCGGGCCATACC 3'	(Macey et al., 1997a)
L4882a1	5' TGACAAAAACTAGCACC 3'	(Macey et al., 1997a)
L4882a2	5' TGACAAAAACTAGCCCC 3'	(Macey et al., 2000)
L4882b	5' TGACAAAAATTGCNCC 3'	(Macey et al., 2000)
L4882c	5' TGACAAAANCTNGCCC 3'	This Study
H4980	5' ATTTCGTTGAGTTGGGTTGRTT 3'	(Macey et al., 1997a)
L5551	5' GACCAAAGGCCCTCAAAGCC 3'	(Macey et al., 1997b)
L5617b	5' AAAGTGTCTGAGTTGCATTCA 3'	(Macey et al., 1997a)
L5638a	5' CTGAATGCAACYCAGAYATTT 3'	(Macey et al., 1997a)
H5692	5' GCGTTTAGCTGTTAACTAAA 3'	(Weisrock et al., 2001)
L5805	5' CGTTGAAATTGCAATYTC 3'	This Study
H5934	5' AGRGTGCCAATGCTTTGTGRTT 3'	(Macey et al., 1997a)
H6159	5' GCTATGTCGGGGCTCCAATTAT 3'	(Weisrock et al., 2001)

and Crandall, 1998) were used to find the model optimal for individual data sets. The resulting models and estimated parameters were used in the maximum-likelihood analyses. Alternative maximum-likelihood phylogenetic topologies were tested using the Shimodaira and Hasegawa (SH) test with 1000 RELL bootstrap replicates (Goldman et al., 2000; Shimodaira and Hasegawa, 1999) as implemented in PAUP* v4.0. This included the same a priori hypotheses tested under parsimony, as well as two a posteriori hypotheses based on the topologies of the ML and Bayesian trees. Alternative topologies were generated using maximum likelihood as described above for the Wilcoxon signed-ranks test. To determine whether individual branches in the resulting ML tree were significantly different from zero, we used a likelihood-ratio test as implemented in PAUP* v4.0 following Slowinski (2001) with a mixed chi-square distribution (Goldman and Whelan, 2000).

Bayesian phylogenetic analysis (Huelsenbeck et al., 2001; Larget and Simon, 1999; Yang and Rannala, 1997) was performed on the individual mtDNA and nuclear rRNA data sets and on combined molecular and morphological data sets using the parallel-processor version of MrBayes v3.04 (Altekar et al., 2004; Huelsenbeck and Ronquist, 2001) run on a Silicon Graphics Origin 2000 through the Washington University Center for Scientific Parallel Computing (<http://harpo.wustl.edu>). In all analyses four Markov chains were used with the temperature profile at the default setting of 0.2.

In Bayesian analyses of combined data sets we used a partitioned model (Nylander et al., 2004). Combined molecular data analyses treated the mtDNA and nuclear rRNA as separate partitions, using appropriate models

as determined through likelihood-ratio tests. Combined molecular and morphological analyses used three partitions and implemented the Lewis Mk model for the morphological data partition (Lewis, 2001).

In all analyses uniform priors were used for all model parameter estimates, and random trees were used to start each Markov chain. For the mtDNA data set, five million generations were run with a tree sampled every 5000th generation for a total of 1000 trees. For the rRNA data set, 10 million generations were run with a tree sampled every 5000th generation for a total of 2000 trees. For all combined analyses two million generations were run with a tree sampled every 1000th generation for a total of 2000 trees. All saved trees from generations prior to a stationary likelihood value were discarded. Trees in the posterior distribution were parsed with MrBayes to construct phylogenograms based upon mean branch lengths and with PAUP* v4.0 to calculate the posterior probabilities of all branches using a majority-rule consensus tree. To account for the possibility that individual analyses may not converge upon the stationary posterior distribution, two additional independent runs were performed for each data set using identical conditions. Likelihood values, tree topology, branch lengths, and posterior probabilities were compared across the replicated runs to verify that similar results were achieved.

For both molecular data sets, maximum-likelihood and Bayesian analyses reconstructed the same tree topology. Consequently, Bayesian posterior probabilities were indicated on the maximum-likelihood tree. Bayesian posterior probabilities equal to or greater than 0.95 indicate statistically significant branch support. Therefore, we treat posterior probabilities as statistical measures

and apply this test to the same alternative hypotheses tested with the WS-R and SH tests. Use of Bayesian posterior probabilities as measures of phylogenetic support is a contentious issue because a number of studies suggest that it gives overconfidence under some conditions (e.g., Simmons et al., 2004; Suzuki et al., 2002; Waddell et al., 2001). In contrast, simulation studies suggest that Bayesian analysis provides reliable results (e.g., Alfaro et al., 2003; Wilcox et al., 2002).

Mitochondrial-DNA Simulations

DNA-sequence simulations were performed to examine the combined influences of the length of an internal branch and its phylogenetic depth on its recovery with significant decay indices in a parsimony analysis and with high posterior probabilities in a Bayesian analysis. We chose three subsets of salamander taxa from the mtDNA phylogeny for the mtDNA simulations. Each subset contained three confamilial ingroup species whose relationships were robustly supported in the mtDNA analysis and a single outgroup from another salamander family (Fig. 1). Branch lengths were estimated for each four-taxon subset individually using maximum likelihood. Evolutionary models that best fit the individual data sets were assessed using likelihood-ratio tests as described above for the larger data sets.

We generated topologies for simulation of DNA evolution (Fig. 2) using two forms of branch-length manipulation. First, we started with the initial ML phylogram for each subset of taxa and successively shortened the internal branch (y) by a length of 0.0032 in units of likelihood-corrected sequence divergence. This procedure produced a series of trees with shortened internal branches (Fig. 2, moving from left to right). Each time branch y was shortened, an equivalent length was added to the terminal branches z_1 and z_2 to preserve overall tree height. Reduction of the internal branch was repeated until the tree formed a polytomy. Because initial branch lengths differed among the three model trees (Fig. 1), some trees needed more rounds of internal-branch shortening than others to reach a polytomy. Second, for each

tree generated in this manner, a new series of trees was created to adjust the depth of the internal branch by successively increasing the lengths of all terminal branches (w , x , z_1 , and z_2) by 0.0032 (moving from top to bottom in Fig. 2). For each set of taxa, this lengthening of terminal branches was repeated for the same number of steps needed to reduce branch y to a polytomy. The end product of these manipulations was a large set of trees representing the starting phylogram and all pairwise combinations of a reduction in length of y and an increase in phylogenetic depth of the internal branch (Fig. 2). For each tree, 100 replicate data sets of 1829 base pairs (the total number of included mtDNA base pairs in the empirical analyses) each were simulated in Seq-Gen v1.2.3 (Rambaut and Grassly, 1997) using the model parameters that best fit the particular four-taxon data set.

All data sets were analyzed by parsimony in PAUP* v4.0 using the exhaustive-search option. For each replicate data set the decay index for the branch uniting the two most closely related ingroup taxa was calculated. For simulated data sets in which the true phylogeny was not the shortest recovered tree, the decay index was scored as zero. The significance of the decay index for each replicate data set was determined via the four-taxon test of Felsenstein (1985) based on the number of phylogenetically informative characters for each simulation. Significance values for decay indices depend on expectations of a molecular clock. Using likelihood-ratio tests, we did not reject a molecular clock for our three starting four-taxon ML trees; therefore, we used significant decay-index values that assumed a molecular clock (Felsenstein, 1985; Weisrock et al., 2001). The percentage of significant decay indices from 100 replicate simulated data sets was calculated for each tree. These data were then plotted as a function of the length of the internal branch and the depth of the internal branch in the phylogeny.

Lack of automation precluded Bayesian analysis of all replicate data sets for all trees. Therefore, for each of the three four-taxon subsets we analyzed 10 simulated data sets from each of 25 trees spaced evenly among the full set of manipulated trees. Bayesian analysis was performed

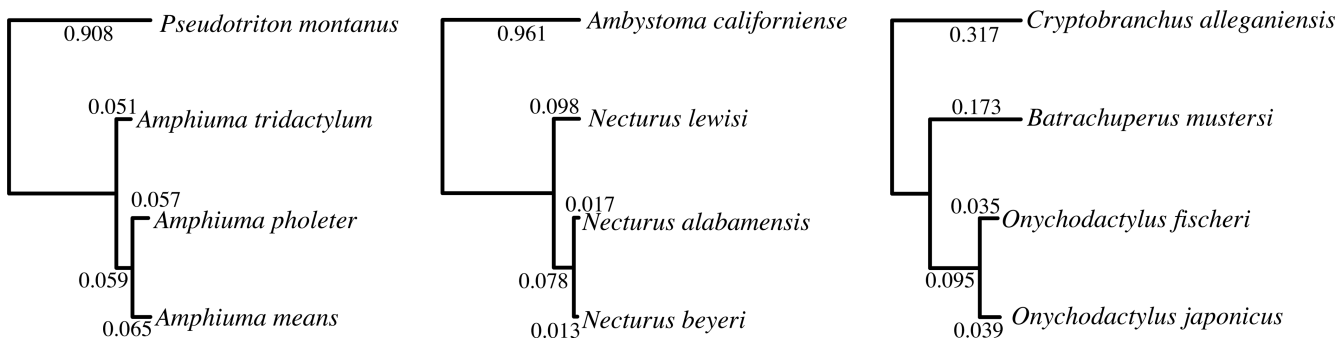


FIGURE 1. Topologies and branch lengths for the three four-taxon subsets used in simulations of mtDNA data. These include three species of *Amphiuma* from the family Amphiumidae and a plethodontid outgroup, three species of the genus *Necturus* from the family Proteidae and an ambystomatid outgroup, and three hynobiid species with a cryptobranchid outgroup. The three groups represent subsets of taxa that were strongly supported in the parsimony analysis of the full mtDNA data set. Numbers along branches represent maximum-likelihood branch lengths using the evolutionary models determined for each individual data set (Table 3).

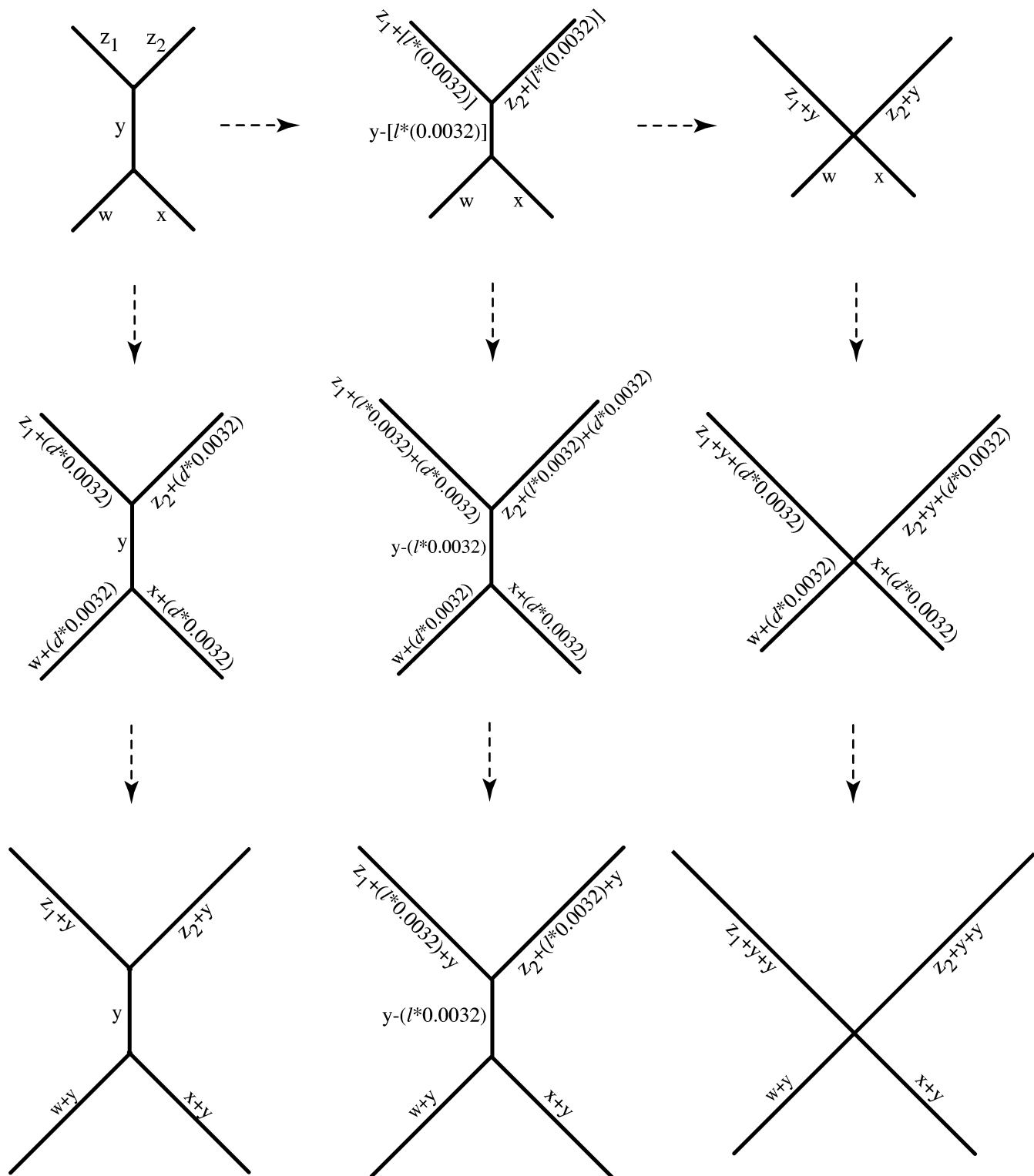


FIGURE 2. Schematic diagram of the generation of trees used in the mitochondrial DNA simulations. The starting tree is represented in the upper left corner of the figure. To decrease the length of the internal branch (branch y , moving from the upper left corner to the upper right corner), a series of trees is generated by successively reducing y by increments (l) of 0.0032 for the number of steps required to reach a polytomy. In each round of shortening, a length of 0.0032 is added to the two terminal ingroup branches, z_1 and z_2 . From each tree generated in this manner, a new series of trees is made to push the internal branch deeper into the phylogeny by successively adding branch-length increments (d) of 0.0032 to every terminal branch (moving top to bottom in the figure). This procedure is repeated the same number of times needed to reduce the internal branch to a polytomy.

as described above using one million generations with a burnin of 100,000 generations. The average posterior probability for the internal branch of each tree was plotted in the same fashion as the decay indices.

The ND1-COI gene region used in this study has been shown to evolve at a consistent rate in numerous vertebrate groups (Bermingham et al., 1997; Hrbek and Larson, 1999; Macey et al., 1998a, 1999), including salamanders (Weisrock et al., 2001), which exhibit a per-lineage rate of approximately 0.64% change per million years (My). We therefore used this calibration for interpreting the simulations in evolutionary time.

Analysis of Likelihood-Based Character Change

We examined the character changes that support branches in the mtDNA likelihood-based trees. Two deep interfamilial branches that were not recovered using parsimony but had significant posterior probabilities (branches A and B) were compared to a deep interfamilial branch that was not recovered using parsimony (branch C) and had a low posterior probability (<0.5). For each branch, the maximum-likelihood tree was compared to alternative trees found through a maximum-likelihood search constrained not to contain the branch under consideration. The log-likelihood ($\ln L$) value was calculated for each character position in the mtDNA data for each tree being compared. For the 25 positions that showed the greatest difference in $\ln L$ favoring the original maximum-likelihood tree, we identified the types of substitutional change that differed between the two trees according to maximum-likelihood reconstructions of character change obtained from the "Describe Trees"

option in PAUP*. For each of the 25 positions we also calculated the gamma-shape-approximation rate category that received the highest posterior probability. The gamma-shape approximation was divided into quartiles with quartile one representing characters with the lowest probability of change and quartile four representing characters with the highest probability of change.

RESULTS

Nuclear rRNA Phylogeny

The nuclear rRNA data set contains 2819 aligned positions, of which 77 are excluded because of ambiguous alignment (positions 701–705, 874–885, 2109–2160, and 2408–2415). The remaining 2743 characters contain 2547 invariant positions, 68 phylogenetically uninformative positions, and 128 phylogenetically informative positions. Likelihood-ratio tests of alternative evolutionary models select the General Time-Reversible model GTR + I + Γ as the one that best fits the nuclear rRNA data (Table 3). Plots of absolute numbers of substitutions against ML corrected sequence divergences reveal a linear pattern indicating that there is little substitutional saturation in the rRNA data.

Parsimony analysis produces four most-parsimonious trees of 317 steps (results not shown). Maximum-likelihood analysis produces essentially the same phylogenetic topology with a $\ln L$ of -5701.07 (Fig. 3). Differences between the parsimony and ML topologies are restricted to short branches within the families Hynobiidae and Plethodontidae. Likelihood-ratio tests reveal that two branches in the ML tree are not statistically

TABLE 3. Best-Fit ML models and parameters as determined by likelihood-ratio tests implemented in ModelTest (Posada and Crandall, 1998). Two main models of sequence variation accounted for the different data sets: The General-Time-Reversible (GTR) model of Yang (1994) and the Hasegawa-Kishino-Yano (HKY) model of Hasegawa et al. (1985).

Data set	ML model	Proportion of invariant sites (I)	Gamma-shape parameter	Estimated base frequencies	Ti:Ti ratio	Substitution rate matrix	
Nuclear rRNA ^a	GTR+I+ Γ	0.8304	2.3592	G = 0.3403 A = 0.1978 T = 0.1835 C = 0.2784	—	A-C = 1.6493 A-G = 2.9172 A-T = 0.3969	C-G = 0.9164 C-T = 8.4170 G-T = 1.0000
mtDNA full data set ^a	GTR + I + Γ	0.2237	0.5691	G = 0.0538 A = 0.3888 T = 0.3020 C = 0.2554	—	A-C = 0.2786 A-G = 5.1495 A-T = 0.3106	C-G = 0.6103 C-T = 2.5456 G-T = 1.0000
<i>Amphiuma</i> mtDNA subset ^b	HKY+ Γ	—	0.2560	G = 0.1185 A = 0.3409 T = 0.2770 C = 0.2636	4.3742	—	—
<i>Necturus</i> mtDNA subset ^b	HKY+I	0.5870	—	G = 0.1137 A = 0.3486 T = 0.3319 C = 0.2057	4.7279	—	—
Hynobiidae mtDNA subset ^b	GTR+ Γ	—	0.5138	G = 0.1250 A = 0.3328 T = 0.3327 C = 0.2094	—	A-C = 2.3926 A-G = 7.4781 A-T = 5.2252	C-G = 0.0000 C-T = 14.036 G-T = 1.0000

^aEstimates of parameters calculated as averages from the Bayesian posterior distribution.

^bEstimates of parameters from likelihood-ratio tests implemented in Modeltest (Posada and Crandall, 1998).

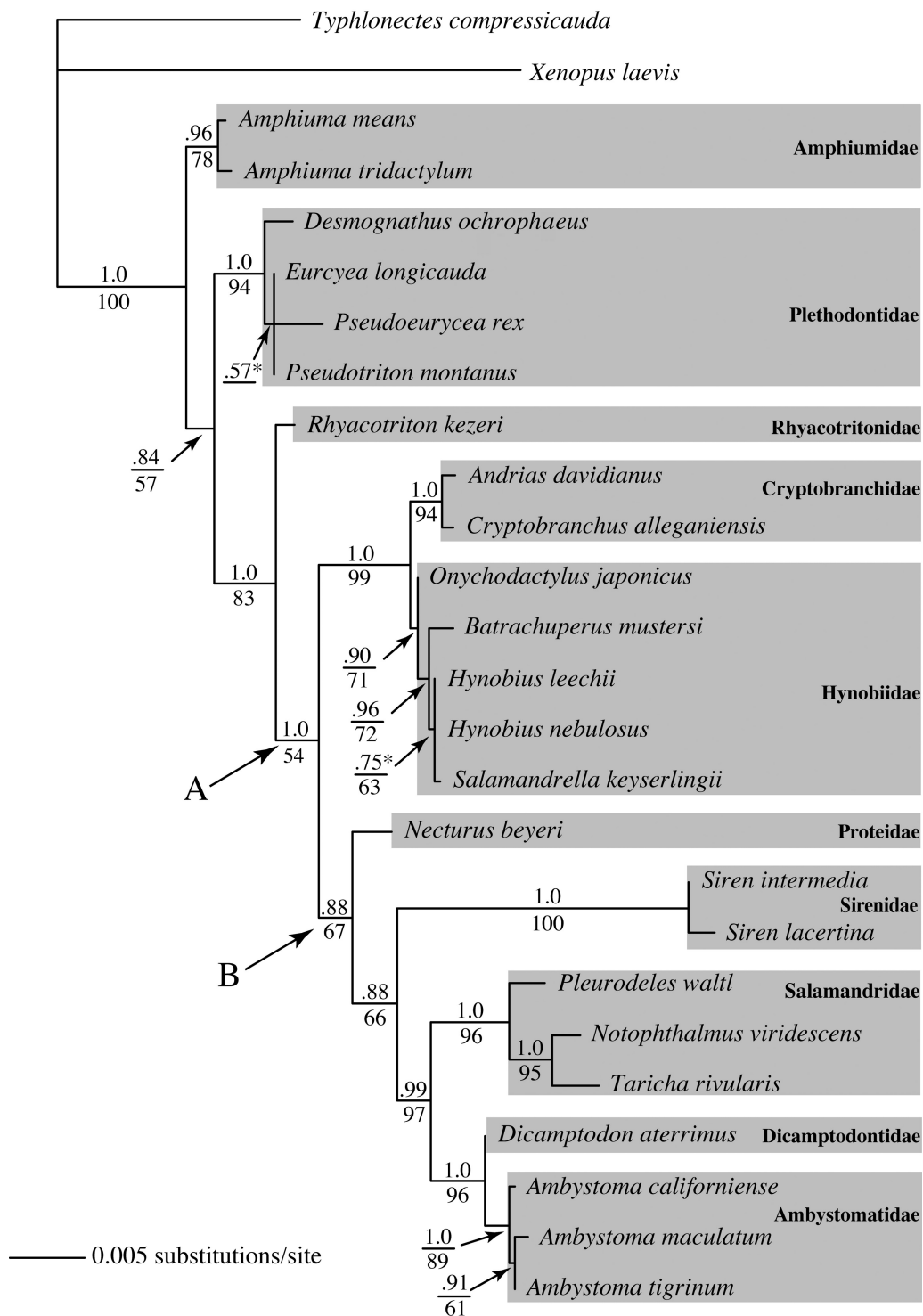


FIGURE 3. Phylogram resulting from maximum-likelihood analysis of the nuclear ribosomal RNA data. The ML topology was similar to the Bayesian and parsimony topology, and their branch-support measures are mapped to the ML phylogram. Numbers above branches represent posterior probabilities calculated from a majority-rule consensus tree of the Bayesian posterior distribution of trees. Numbers below branches represent parsimony bootstrap values above 50%. Branches for which zero length could not be statistically rejected at the $p \leq 0.05$ level are denoted with an asterisk. Two branches (A and B) that show concordance with the mtDNA ML and Bayesian tree are labeled. Shaded boxes denote the individual salamander families.

different from zero length (Fig. 3). However, neither of these branches groups different salamander families. The Bayesian posterior distribution produces a consensus topology almost identical to the parsimony and ML trees. A stationary lnL is reached at approximately 950,000 generations with a mean lnL of -5738.27, a maximum of -5718.29, and a variance of 53.79. For a conservative analysis, all trees from generations one through 1,000,000 are discarded. Additional Bayesian analyses yield topologically identical results, suggesting that a stationary posterior distribution is reached (results not presented).

The sister-taxon relationship of Hynobiidae and Cryptobranchidae is strongly supported by parsimony and Bayesian analysis (bootstrap 99%, PP 1.0; Fig. 3). An alternative topology without this grouping is rejected by the WS-R test and by Bayesian criteria, but it is not rejected by the SH test (Table 4). The sister-taxon relationship of Ambystomatidae and Dicamptodontidae is strongly supported by parsimony and statistically supported by the Bayesian analysis (bootstrap 96%, PP 1.0; Fig. 3). Alternative topologies without this grouping are not rejected by the Wilcoxon signed-ranks test or the SH test; however, the *P*-values of both tests approach significance (Table 4). Placement of Salamandridae as the sister taxon to the ambystomatid and dicamptodontid clade is also strongly supported by both parsimony and Bayesian analyses (bootstrap 96%, PP 1.0; Fig. 3). However, alternative topologies in which these three families do not form a clade cannot be rejected statistically by the WS-R and SH tests (Table 4).

Monophyly of the internally fertilizing suborder Salamandroidea is statistically rejected using Bayesian crite-

ria, but it is not rejected under the WS-R and SH tests (Table 4). All analyses place Amphiumidae, Plethodontidae, Rhyacotritonidae, and a clade comprising the remaining families as deep branches in salamander phylogeny. Furthermore, Amphiumidae is consistently placed as the sister taxon to all remaining salamander families across all analyses of the nuclear data set. Relationships among these four branches are not resolved with strong support by parsimony (Fig. 3), but the Rhyacotritonidae is strongly supported as the sister taxon to a clade containing all remaining families except for Amphiumidae and Plethodontidae with Bayesian posterior probabilities of 1.0 (Fig. 3).

Mitochondrial DNA Phylogeny

Alignment of mtDNA sequences produces a character matrix of 2115 base pairs, of which 286 positions are excluded because of ambiguous alignment (positions 154–183, 376–388, 402–408, 431–435, 441–448, 461–467, 518–525, 539–545, 558–563, 595–601, 867–908, 1638–1664, 1678–1683, 1715–1721, 1734–1744, 1757–1763, 1813–1819, 1832–1838, 1871–1878, 1892–1901, 1911–1932, 1956–1962, 1968–1972, 1995–1999, 2013–2014, 2027–2033, 2065–2070, and 2084–2085). The multiple alignment contains 555 invariant characters, 152 parsimony-uninformative characters, and 1122 parsimony-informative characters. Likelihood-ratio tests of alternative evolutionary models select the GTR + I + Γ model as optimal for the mtDNA data (Table 3). Plots of absolute numbers of substitutions against ML-corrected sequence divergences reveal patterns consistent with substitutional saturation

TABLE 4. Parsimony and maximum likelihood-based statistical tests of alternative topologies. All probabilities are based on a one-tailed distribution. A significant result denotes rejection of the alternative hypothesis. Some tests assess significance of branches that are found in the mtDNA ML tree, but not in the mtDNA parsimony tree. Clades A and B are as denoted in Figures 3 and 4b.

Data set	Alternative topology tested	Probability WS-R test ^a	Bayesian criterion ^b	$\Delta \text{LnL}^{\text{c}}$	Probability SH test ^d
Nuclear rRNA	Without monophyletic Caudata	<i>P</i> < 0.002*	<i>P</i> = 0.0*	-6.18	<i>P</i> = 0.085
	With monophyletic Salamandroidea	<i>P</i> < 0.238	<i>P</i> = 0.0*	-14.452	<i>P</i> = 0.1
	Without monophyletic Cryptobranchoidea	<i>P</i> < 0.017*	<i>P</i> = 0.0*	-12.303	<i>P</i> = 0.126
	Without Ambystomatidae + Dicamptodontidae	<i>P</i> < 0.078	<i>P</i> = 0.0*	-17.038	<i>P</i> = 0.052
	Without Ambystomatidae + Dicamptodontidae + Salamandridae	<i>P</i> < 0.078	<i>P</i> = 0.01*	-14.83	<i>P</i> = 0.088
	Without Clade A			-6.958	<i>P</i> = 0.137
	Without Clade B			-5.693	<i>P</i> = 0.111
mtDNA	Without monophyletic Caudata	<i>P</i> = 0.020*	<i>P</i> = 0.0*	-45.554	<i>P</i> = 0.013*
	With monophyletic Salamandroidea	<i>P</i> < 0.011*	<i>P</i> = 0.0*	-21.176	<i>P</i> = 0.135
	Without monophyletic Cryptobranchoidea	<i>P</i> < 0.193	<i>P</i> = 0.0*	-11.985	<i>P</i> = 0.200
	With monophyletic Proteidae	<i>P</i> = 0.049*	<i>P</i> = .053	-3.379	<i>P</i> = 0.389
	Without Clade A	—	<i>P</i> = 0.0*	-15.808	<i>P</i> = 0.184
	Without Clade B	—	<i>P</i> = 0.0*	-10.006	<i>P</i> = 0.240

^aParsimony-based Wilcoxon signed-ranks test using a one-tailed probability (Templeton, 1983).

^bThe proportion of trees in the Bayesian posterior distribution that contained the alternative phylogenetic topology.

^cThe difference in the lnL score between the alternative ML tree and the unconstrained ML tree.

^dLikelihood-based SH test using a one-tailed probability (Shimodaira and Hasegawa, 1999).

*Significant difference at *P* < 0.05 in columns 3, 4, and 6.

in the mtDNA protein-coding regions but not in tRNA genes.

Parsimony analysis of the mtDNA data produces a single most parsimonious tree of 8285 steps (Fig. 4a). Maximum-likelihood analysis produces an optimal tree

with a lnL score of -33,780.27 (Fig. 4b). Bayesian analysis produces a phylogenetic topology identical to the ML tree. A stationary lnL occurs after approximately 55,000 generations with a mean lnL of -33,799.71, a maximum of -33,782.28, and a variance of 54.3. For a conservative

(a) mtDNA Parsimony

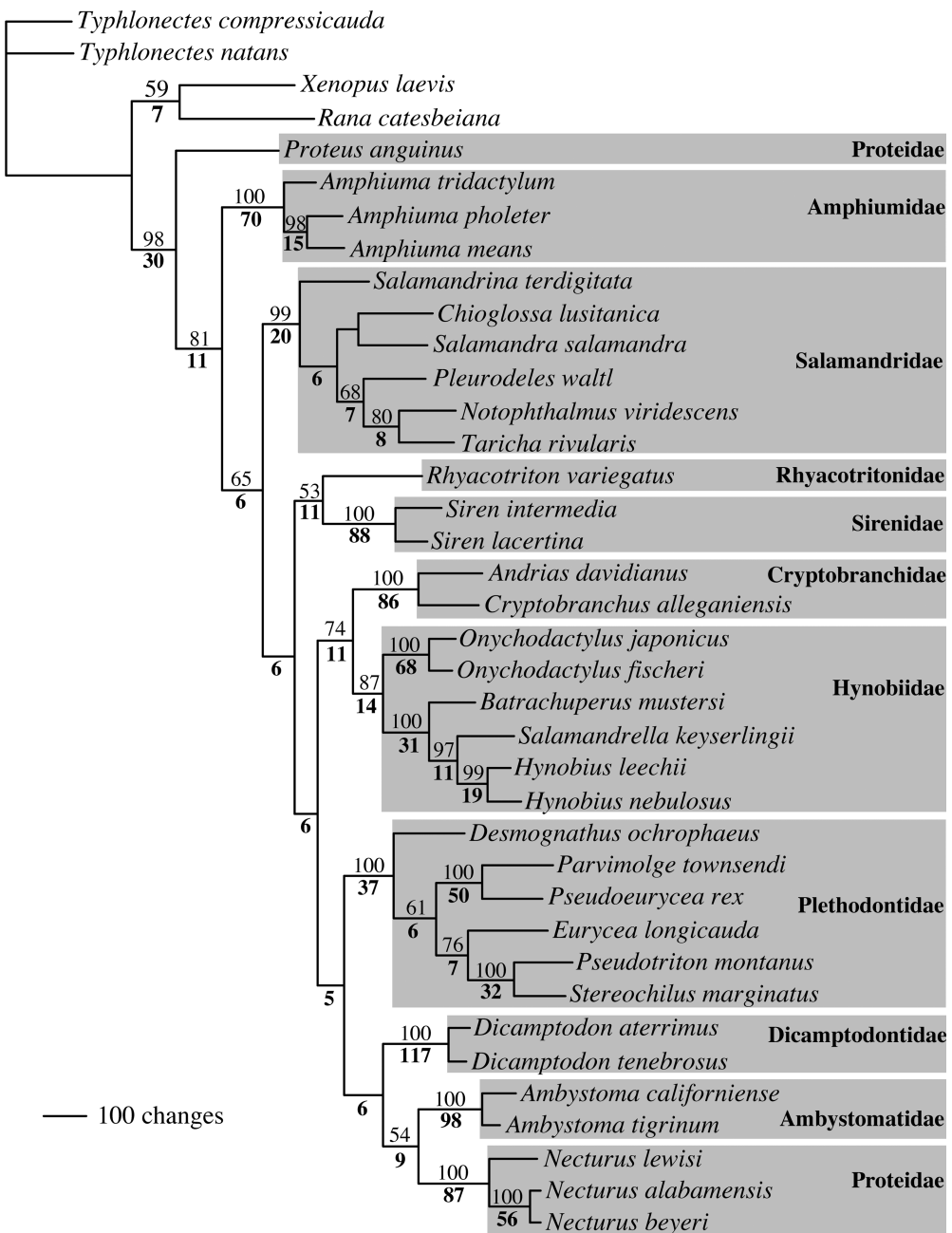


FIGURE 4. (a) Single most-parsimonious tree of 8285 steps resulting from analysis of mtDNA sequence data. Numbers above branches represent bootstrap values above 50%, and numbers below branches represent decay indices. (b) Maximum-likelihood phylogram resulting from analysis of the mtDNA sequence data. Numbers on branches represent posterior probabilities calculated from a majority-rule consensus tree of the Bayesian posterior distribution of trees. Branches whose length is not statistically different from zero at the $P \leq 0.05$ level are marked with asterisks. Branches A and B are deep interfamilial branches that have a significant Bayesian posterior probability, are not reconstructed in the parsimony analysis, but are concordant with branches resolved in analyses of the nuclear rRNA. Branch C represents a relatively deep relationship not recovered with significant posterior probability (and also not recovered using parsimony) and is used for comparison to A and B in analyses of character change. Shaded boxes correspond to the individual salamander families. (Continued)

(b) mtDNA ML/Bayesian

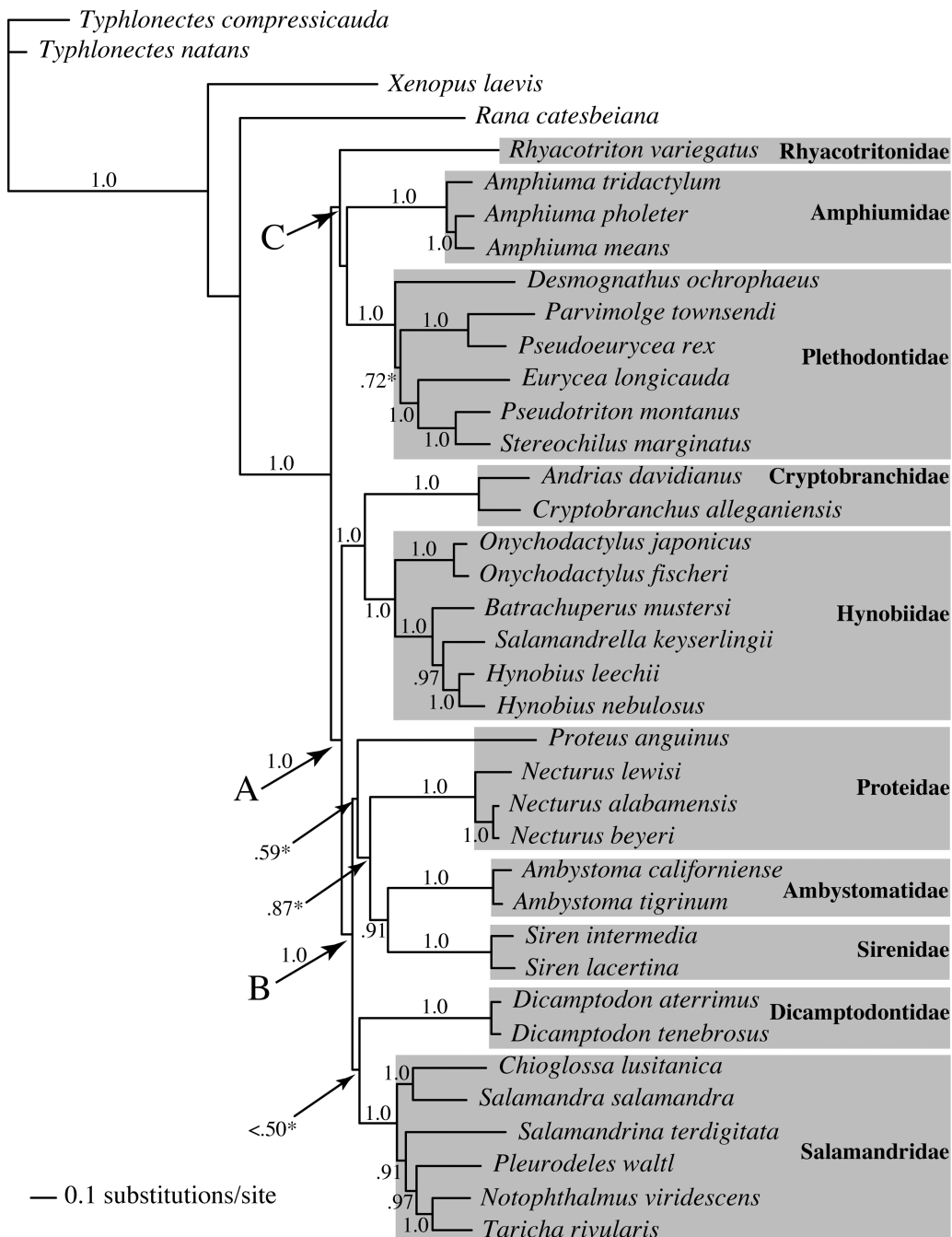


FIGURE 4. Continued.

analysis, all trees from generations one through 100,000 are discarded. Replicated Bayesian analyses yield identical results, suggesting that the optimal posterior distribution is reached (results not presented).

A monophyletic Caudata is strongly supported in both the parsimony and Bayesian analyses (bootstrap 98%; decay index 30; PP 1.0; Fig. 4a, b). Alternative topologies without this relationship are rejected using all statistical

tests (Table 4). All analyses produce topologies inconsistent with monophyly of internally fertilizing salamanders (Fig. 4a, b). A monophyletic Salamandroidea is rejected using the WS-R tests and under Bayesian criteria but not by the SH test (Table 4).

Except for Proteidae, all families with multiple representatives form strongly supported monophyletic groups in all analyses (Fig. 4a, b). These results are

particularly noteworthy for family Hynobiidae, whose monophyly has been questioned (Trueb, 1993). Branch support in the parsimony tree for relationships among salamander families is low. The clade comprising Cryptobranchidae and Hynobiidae receives the strongest support in the parsimony tree (bootstrap 74%; decay index 11) (Fig. 4a). Alternative topologies without this relationship are not rejected statistically by the WS-R test (Table 4).

Branches grouping salamander families in the ML tree are short relative to branches immediately ancestral to individual families. Likelihood-ratio tests reveal four branches not statistically different from zero length (Fig. 4b). Three of these zero-length branches represent deep interfamilial relationships. However, posterior probabilities assigned to three of the nodes in the mtDNA Bayesian tree show statistical support ($PP = 1.0$) for interfamilial relationships (Fig. 4b; Table 4): (1) a clade comprising Ambystomatidae, Sirenidae, Proteidae, Salamandridae, and Dicamptodontidae (labeled branch B in Fig. 4b); (2) a clade composed of the Cryptobranchidae and Hynobiidae; and (3) a clade comprising the above two groups (labeled branch A in Fig. 4b). Tests of alternative ML topologies lacking branches A and B and the Cryptobranchidae-Hynobiidae clade are not statistically rejected by the SH test (Table 4).

Monophyly of family Proteidae is not recovered in our analyses. The European species, *Proteus anguinus*, forms the sister taxon to a group containing all remaining salamanders in the parsimony tree (Fig. 4a). In the likelihood-based analyses, *Proteus anguinus* forms the sister taxon to a clade comprising *Necturus* and families Ambystomatidae and Sirenidae; however, this relationship does not receive a significant posterior probability, and the branch immediately ancestral to this group is not statistically different from zero length (Fig. 4b). An alternative topology in which *Proteus anguinus* and genus *Necturus* are united to form a monophyletic family Proteidae is statistically rejected by the Wilcoxon signed-ranks test but not by the SH test (Table 4). Rejection of this alternative hypothesis approaches significance using Bayesian criteria (Table 4). Recent studies using partial 12S mtDNA sequences (Trontelj and Goricki, 2003) and RAG-1 sequences (Wiens et al., 2005) support monophyly of Proteidae, although only the latter analysis seems statistically robust.

Kumazawa and Nishida (1993) suggest that the slower evolution of mtDNA tRNA stems might provide phylogenetic information for deep phylogenetic relationships, and they provide convincing examples of recovery of deep animal relationships with strong branch support. Parsimony analysis of the eight mitochondrial tRNA stem sequences yields 29 trees of 1171 steps in length. A strict consensus of these trees produces a large polytomy and fails to recover monophyly of the families Salamandridae and Hynobiidae (results not shown), clades strongly supported in the total-mtDNA parsimony analysis. Thus, restricting the analysis to slower-evolving sites in tRNA genes does not enhance deep phylogenetic resolution.

Combined Analyses

Partitioned Bayesian analysis of a combined mtDNA and nuclear rRNA data matrix using complete taxon sampling produces a tree with an average lnL of -39814.18 , a maximum of -39794.51 , and a variance of 51.52 (Fig. 5). This tree is nearly identical to a tree produced from a tripartitioned Bayesian analysis of a combined mtDNA, nuclear rRNA and morphological data matrix, which had an average lnL of -40172.87 . A stationary distribution is reached in both analyses by the 25,000th generation, and the first 100,000 generations are treated as burn-in. The combined-data Bayesian trees are very similar to the trees produced in Bayesian analysis of the individual molecular data sets and find strong support for all interfamilial relationships supported in the single-partition trees. However, the combined trees provide increased support for the most basal interfamilial branching event between the Amphiumidae and a clade containing all remaining salamander families (Fig. 5). The only uncertain family-level relationships are the exact placement of lineages representing the Proteidae (*Necturus* and *Proteus*) and Sirenidae. However, these families are firmly placed within the clade identified by branch B in the individual molecular Bayesian trees. There was no appreciable difference in results between combined-data analyses using all taxa from all data sets and combined-data analyses using a pruned taxon sampling (results not shown).

Parsimony analysis of the full-taxa, combined morphological and molecular data matrix produces a single tree of 10221 steps (tree not shown). As in the mtDNA parsimony tree, the combined-data tree places *Proteus anguinus* outside a clade containing the remaining taxa. However, this placement and most other deep internal branches are poorly supported. Only two interfamilial relationships receive bootstrap values greater than 65% in the combined parsimony tree: (1) the clade composed of Cryptobranchidae and Hynobiidae (99%) and (2) the clade composed of Ambystomatidae and Dicamptodontidae (86%). There was no appreciable difference in results between combined-data parsimony analyses using all taxa from all data sets and combined-data analyses using a pruned taxon sampling (results not shown). The sister-group relationship of Ambystomatidae and Dicamptodontidae and their sister-group relationship to the Salamandridae are consistent with phylogenetic results of Titus and Larson (1995) based on mitochondrial genes encoding 12S and 16S rRNA.

Mitochondrial DNA Simulation Results

The relationship between branch lengths, the minimal decay index needed for statistical significance, and Bayesian posterior probabilities show similar patterns across the three separate sets of mtDNA-based simulations. Recovery of both significant decay indices and posterior probabilities decreases as the internal branch (y) moves deeper into the tree and as the length of y is shortened (Fig. 6). However, comparisons across the

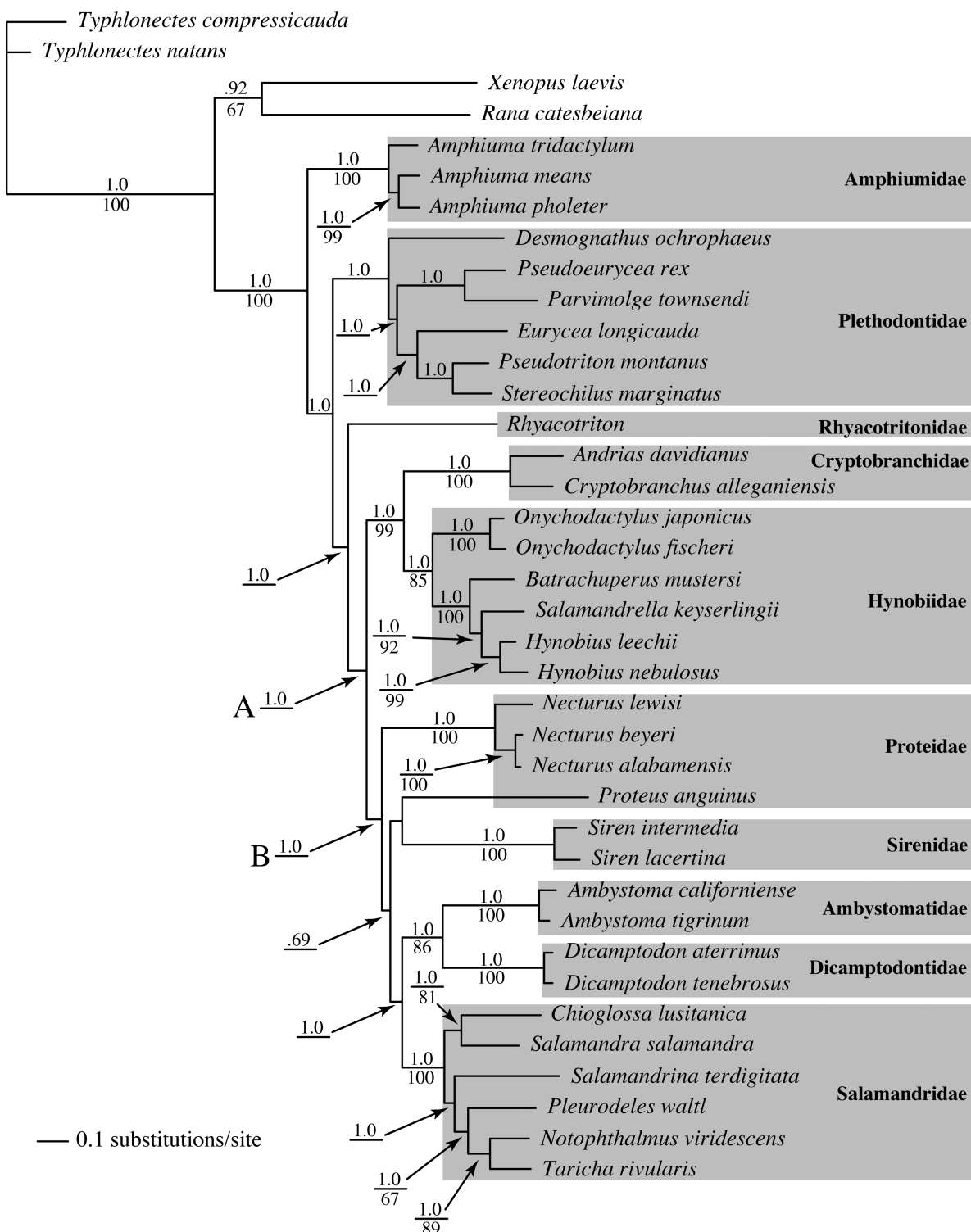


FIGURE 5. Bayesian tree resulting from a combined and tripartitioned analysis of morphology, nuclear rRNA, and mtDNA data. This analysis uses all 38 taxa in the mtDNA data set and codes taxa without morphological or rRNA characters as missing data. The branching structure and posterior probabilities are not different from an approach in which taxa with missing data were excluded from analysis. Numbers above branches represent posterior probabilities, and numbers below branches represent corresponding parsimony bootstrap values. Branches without bootstrap values were either below 50% or not recovered in the parsimony tree. The single representative of the Rhyacotritonidae is not labeled with a species name due to the combined use of rRNA and mtDNA sequence data from different species. Shaded boxes correspond to the individual salamander families. Clades A and B, which are concordantly resolved with strong Bayesian support in the individual mtDNA and rRNA Bayesian and ML analyses, are labeled on the combined tree.

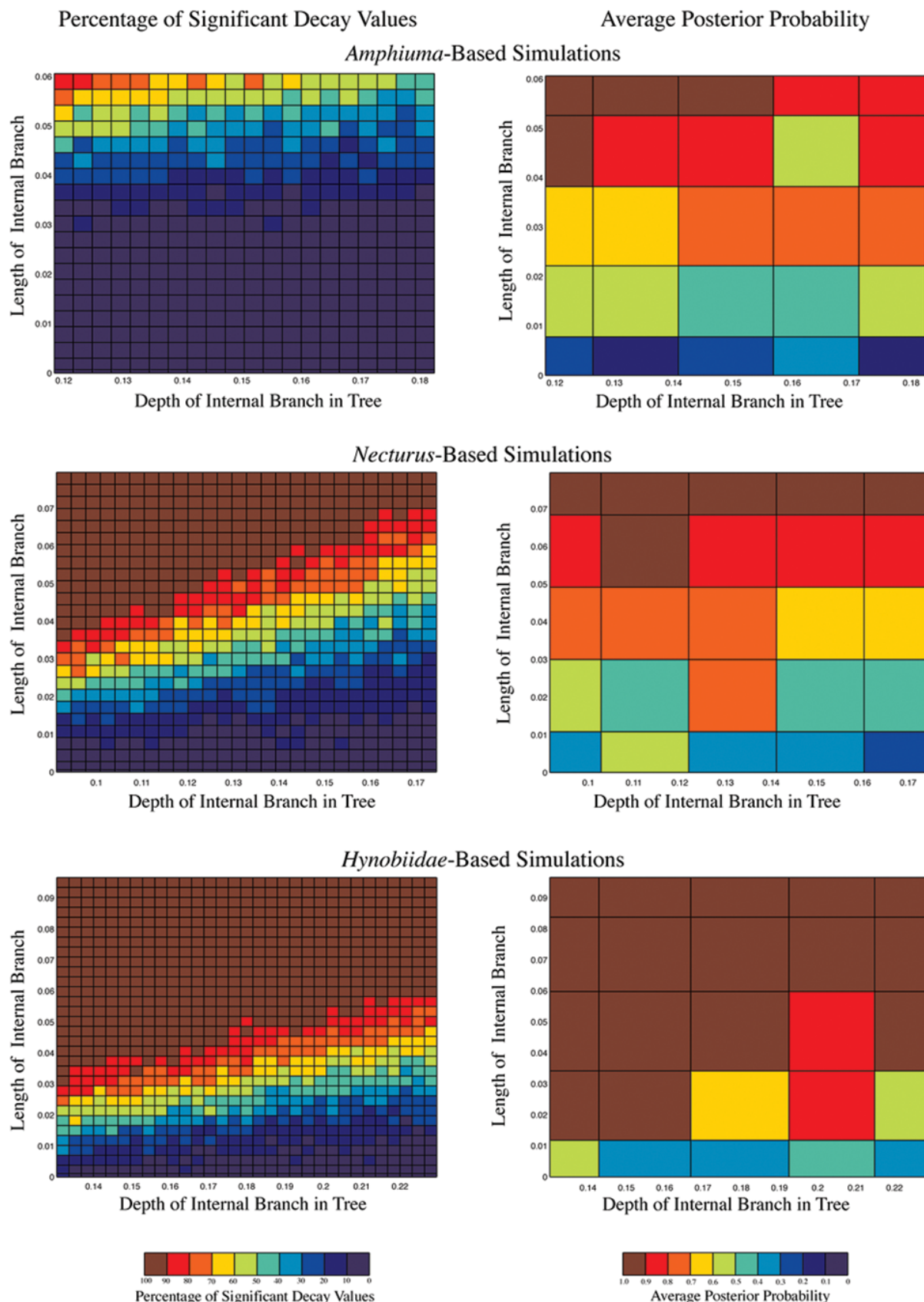


FIGURE 6. Plots of the percentage of significant decay indices in a parsimony analysis (left) and average Bayesian posterior probabilities (right) recovered from replicate simulated data sets as a function of the length of the internal branch (y) and its depth in the phylogeny. All axes are in units of the expected number of substitutions per site.

three sets of simulated trees reveal a consistent pattern of higher statistical power of posterior probabilities relative to decay indices.

Differences in the graphical patterns of Figure 6 are partly a function of differences in branch lengths among the three starting trees. For example, recovery of the true tree from the simulated data sets is higher in the Hynobiidae-based simulations than the *Amphiuma* and *Necturus*-based simulations. The greater power in recovery of the true phylogeny in the Hynobiidae-based simulations probably results from availability of a closer outgroup for this four-taxon subset (Fig. 1). This increased power may be influenced also by use of the more parameter-rich General Time-Reversible model of substitution in this simulation relative to the less complex HKY model used in *Amphiuma* and *Necturus*-based simulations.

Based on the Hynobiidae results, an internal branch must have at least 0.03 substitutions per site to be recovered with significant decay indices in 90% to 100% of the subsets when placed at a phylogenetic depth of 0.13 substitutions per site. Bayesian analysis can recover branches of similar depth with average posterior probabilities of 0.9 to 1.0 when internal branches are greater than approximately 0.015 substitutions per site. When the internal branch is placed at a phylogenetic depth of 0.18 substitutions per site, the internal branch needs to be at least 0.045 in length to be recovered with significant decay indices in 90% to 100% of the subsets. Bayesian analysis of trees with an internal-branch depth of 0.18 substitutions per site can be recovered with posterior probabilities in the 0.9 to 1.0 range when the internal-branch length is at least 0.035 substitutions per site. When the phylogenetic depth of the internal branch increases to 0.23 substitutions per site, the internal branch must have at least 0.06 substitutions per site for recovery with significant decay indices in 90% to 100% of the subsets and at least 0.035 substitutions per site to be recovered with an average posterior probability of 0.9 to 1.0.

Likelihood-Based Character Change for mtDNA Data

MtDNA character support was compared for two deep interfamilial branches receiving significant Bayesian posterior probabilities (branches A and B in Fig. 4b) and an interfamilial branch lacking such support (branch C in Fig. 4b) to identify the kinds of character changes that contribute the strongest evidence favoring clades A and B. For branch A, 20 of the 25 character positions with the highest difference in lnL between the ML tree and the alternative tree have a difference of at least 1.0 (Table 5). The top seven characters have a difference of at least 2.0 (Table 5). For branch B, 23 of the top 25 lnL differences are greater than 1.0, and six characters have a difference of at least 2.0 (Table 6). For branch C, 11 of the highest 25 lnL differences are greater than 1.0 and two are greater than 2.0 (Appendix 2, available at www.systematicbiology.org). Character changes with the highest lnL differences (particularly those with a difference greater than 2.0) usually involve transversions

TABLE 5. Overview of character change for 25 mtDNA sequence positions that show the greatest difference in log likelihood (lnL) between the ML tree and an alternative likelihood tree constrained not to contain branch A (Fig. 4b).

Difference in lnL (ML – Alt.)	Position no.	Coding position ^a	Character change ^b	Gamma quartile ^c
5.971	1470	1st pos.	G to T	2
5.728	1087	2nd pos.	G to C	1
5.109	2058	TYR stem	G to T	1
4.657	916	2nd pos.	C to G	1
3.998	2044	TYR stem	C to A	1
2.762	1038	1st pos.	C to A	3
2.681	1548	1st pos.	A to T	3
1.899	1846	ASN loop	C to A; C to T	2
1.759	368	2nd pos.	T to A; T to C	2
1.359	922	2nd pos.	C to T	1
1.311	1785	ALA stem	C to T	2
1.299	1385	3rd pos.	C to A; C to T	3
1.287	1460	3rd pos.	A to T; T to C	3
1.099	1527	1st pos.	T to C; T to G; T to G	3
1.094	670	2nd pos.	T to C	2
1.047	1579	2nd pos.	C to A	3
1.032	1441	2nd pos.	C to T; C to A; C to T	3
1.030	1020	1st pos.	C to A; C to T	3
1.021	755	3rd pos.	A to T; T to C; T to C	4
1.015	2016	TYR stem	G to A	2
0.997	1059	1st pos.	C to T	2
0.978	834	1st pos.	G to A; A to T	3
0.936	1413	1st pos.	T to A; T to A; T to C	4
0.935	1976	CYS stem	G to A	2
0.860	1549	2nd pos.	A to T; T to C	3

^a1st, 2nd, and 3rd pos. refer to codon positions in protein-coding genes. Stem designation of tRNAs refer to a base that pairs with another base according to tRNA structural models. Loop designation refers to any unpaired base.

^bMaximum-likelihood reconstructions of character changes present on a branch in the ML tree that were absent from the alternative tree.

^cThe gamma-shape approximation rate category with the highest posterior probability for a particular nucleotide position. Sites with a high posterior probability of being in category 1 are among the slowest evolving sites in the data set, while sites having a high posterior probability of being in category 4 are among the fastest evolving.

at character positions with low evolutionary rates, typically in 1st or 2nd codon positions or stem structures of tRNA genes (Tables 5, 6; Appendix 2).

DISCUSSION

Challenges in Deep Phylogenetic Reconstruction

Phylogenetic relationships among salamander families illustrate the analytical challenges inherent to inferring phylogenies in which terminal branches are temporally very long relative to internal ones (Felsenstein, 1978; Huelsenbeck, 1997; 1998). As phylogenetic depth increases relative to the length of an internal branch, characters representing true phylogenetic signal become an increasingly smaller portion of the total informative characters in a data set, and parallel changes along terminal branches increase. Together, these factors increase the difficulty of correctly recovering deep phylogenetic relationships with strong branch support and of statistically rejecting alternative phylogenetic hypotheses. This phenomenon often leads to an interpretation of simultaneous branching among multiple lineages. Under these conditions, it is difficult to distinguish

TABLE 6. Overview of character change for 25 mtDNA sequence positions that show the greatest difference in log likelihood ($\ln L$) between the ML tree and an alternative likelihood tree constrained not to contain branch B (Fig. 4b). See Table 5 for explanations of column headings.

Difference in $\ln L$ (ML–Alt.)	Position no.	Coding position	Character change	Gamma quartile
6.184	1470	1st pos.	G to T	2
4.663	916	2nd pos.	C to G	1
4.048	109	1st pos.	G to T	1
2.988	1038	1st pos.	C to A	3
2.530	1284	1st pos.	G to T	2
2.277	1548	3rd pos.	A to T	3
1.917	1846	ASN loop	A to T; C to T	2
1.788	368	2nd pos.	T to A; T to C	2
1.655	553	MET loop	C to A	1
1.534	1949	CYS stem	G to C	2
1.412	1785	ALA stem	C to T	2
1.366	1385	3rd pos.	C to A; C to T	3
1.298	1460	3rd pos.	A to T	3
1.136	1991	CYS stem	G to A	2
1.122	1527	1st pos.	T to G; T to G	3
1.112	755	3rd pos.	A to T	4
1.070	1020	1st pos.	C to A	3
1.063	750	1st pos.	C to A	2
1.044	670	2nd pos.	T to C	2
1.031	1579	2nd pos.	C to A	3
1.030	331	1st pos.	T to A; A to C	3
1.019	2016	TYR stem	G to A	2
1.015	645	1st pos.	A to T	2
0.997	536	GLN stem	C to T	1
0.994	1550	3rd pos.	A to T; T to C	3

analytical artifacts that yield polytomous trees (called a “soft” polytomy) from evolutionarily simultaneous branching of multiple lineages (a “hard” polytomy *sensu* Maddison [1989]).

Our simulations address the phylogenetic resolving power of our mtDNA data and phylogenetic methods using evolutionary models derived from the data to simulate sequence evolution on trees whose internal and terminal branches vary in length. Our mtDNA-based simulations quantify the positive relationship between the evolutionary depth of an internal branch in a phylogenetic tree and the minimum evolutionary duration needed for its recovery with strong branch support (see also Halanych, 1998 and Philippe et al., 1994).

Our results suggest that the mtDNA data have limited ability to recover relatively old and short branches and may not provide substantial support for many branching events deep in salamander phylogeny. Lineages ancestral to groupings of two or more salamander families have a phylogenetic depth of at least 50 million years and possibly as large as 150 million years (reviewed in Larson, 1991; Gao and Shubin, 2001; 2003). Model-based phylogenetic analyses are expected to be more effective in detecting relatively short branches with statistical significance than is unweighted parsimony analysis in four-taxon tests (Hillis et al., 1994; Hulesenbeck, 1995). Our Hynobiidae-based simulations, interpreted using a rough molecular clock calibrated for our mtDNA gene region, suggest that with ~1800 base pairs of aligned sequences, a lineage ancestral to taxa separated for 35

million years (branch length of 0.23 substitutions/site) must be at least 9 million years in duration to be recovered under parsimony with statistically significant decay indices 90% of the time and at least 5 million years in duration on average to be recovered with Bayesian posterior probabilities of 0.9 to 1.0. Ancestral lineages of even half these durations are much less likely to be recovered with strong support (Fig. 6). From these calculations, it seems clear that internal branches ancestral to salamander family lineages would need to have had substantial evolutionary durations to have generated sufficient phylogenetic signal in mtDNA sequences.

These estimates assume roughly constant nucleotide substitution rates over time and that appropriate outgroups are available; they are underestimates of the duration needed for recovery of an ancestral lineage if only very distant outgroups are available. Increased taxon sampling (Hillis, 1996; Poe, 2003; Poe and Swofford, 1999) and closely related outgroups (Halanych et al., 1999) should increase resolving power relative to the conditions simulated. However, increased taxon sampling across salamanders may have limited ability to reduce problems of long-branch attraction because the extant diversity found within salamander families generally represents only a small portion of the total evolutionary duration of a family-level branch. Consequently, even ancestral lineages of substantial evolutionary duration may be very difficult to resolve with confidence if they occur deep in a phylogenetic tree. This analytical problem may be avoided by using sequences that evolve more slowly than the ones modeled (e.g., nuclear rRNA versus mtDNA) due to the slower accumulation of misleading information. However, phylogenetic signal would be diminished proportionately and could substantially limit the resolution of short internal branches (Donoghue and Sanderson, 1992; Fishbein et al., 2001).

Substantial evolutionary changes in morphology and geographic distribution could have occurred early in the evolutionary history of salamanders on ancestral branches that are of millions of years in duration. However, unless these branches were of a minimum duration that could generate sufficient phylogenetic information to withstand long periods of terminal evolution, they would be nearly invisible to currently available phylogenetic methods and could be perceived as a rapid branching event.

Rapid Cladogenesis of Salamander Families?

Short internal branch lengths are frequently highlighted as potential “radiations” of lineages, often with the connotation that cladogenesis occurred simultaneously among multiple lineages. Although the evidence for such radiations has grown (e.g., Schlüter, 2000), only recently have rigorous tests been applied to discriminate hard and soft polytomies (e.g., Fishbein et al., 2001; Jackman et al., 1999; Misof et al., 2001; Poe and Chubb, 2004; Slowinski, 2001; Walsh et al., 1999). Likelihood-ratio tests of nonzero branch lengths (Slowinski, 2001) offer a computationally simple way to test the null

hypothesis of nonzero branch lengths. Such tests may be conservatively biased because only a single branch is allowed to vary between trees (the potentially zero-length branch). Alternative methods such as the parametric bootstrap may offer a more powerful test of nonzero branch lengths (Fishbein et al., 2001; Knowles, 2000; Poe and Chubb, 2004). However, rejection of nonzero branch lengths using a likelihood-ratio test represents robust evidence for the presence of a particular internal branch.

Perhaps the most crucial aspect in diagnosis of a hard polytomy among lineages is the signature of nonzero branch lengths in molecular phylogenies of multiple unlinked loci (Poe and Chubb, 2004; Slowinski, 2001). Using likelihood-ratio tests, we could not reject the hypothesis of zero branch length for three interfamilial branches in the salamander mtDNA ML tree; however, these same branches were found with statistical support in the rRNA ML tree. The mtDNA branch-length patterns are less likely to have arisen as a result of a multifurcating gene tree and are more likely a function of the long time since cladogenesis among salamander families. A major benefit of incorporating our simulation work into our assessment of rapid branching patterns is that it gives us insight into the phylogenetic patterns expected for resolving deep relationships. Decay of phylogenetic signal in our mtDNA data at deep branches during the long evolutionary time since cladogenesis offers the best explanation for zero-length branches deep in the mtDNA ML tree.

Salamander Phylogeny and Potentially Misleading Effects of Weighting Saturated Data

Parsimony analysis of the newly reported mitochondrial genomic sequences provides strong independent support to a number of groupings consistent with prior analyses of nuclear genomic data and morphological characters (Larson et al., 2003; Wiens et al., 2005). These groupings span a large scale of salamander phylogenetic history and include (Fig. 4a) monophyly of (1) Urodela, (2) family Ambystomatidae, (3) family Amphiumidae, (3) family Cryptobranchidae, (4) family Dicamptodontidae, (5) family Hynobiidae, (6) family Plethodontidae, (7) family Salamandridae (8) family Sirenidae, (9) genus *Necturus*, (10) bolitoglossine plethodontids (represented here by *Parvimolge* and *Pseudoeurycea*), (11) hynobiid genus *Onychodactylus*, and (12) hynobiid salamanders excluding genus *Onychodactylus*. Model-based analyses (maximum likelihood, Bayesian analysis) provide strong support to these same groupings (Fig. 4b). As expected from our simulations, model-based analyses demonstrate stronger resolving power in finding statistical support for some additional groupings that received only weak support from the parsimony analysis: (1) monophyly of hemidactyline plethodontids (represented here by *Eurycea*, *Pseudotriton*, and *Stereochilus*); (2) monophyly of Cryptobranchidae (Cryptobranchidae and Hynobiidae); (3) grouping of North American newts *Notophthalmus* and *Taricha* relative to other salamanders; (4) grouping of newts *Notophthalmus*, *Pleu-*

rodeles, and *Taricha* relative to other salamanders; and (5) grouping of true salamanders (*Chioglossa* and *Salamandra*) relative to other salamanders. Only the grouping of *Hynobius* and *Salamandrella* seems stronger in the parsimony analysis than in the Bayesian analysis (Fig. 4).

Several results indicate that most branches grouping two or more salamander families are relatively short ones located deep in the evolutionary history of salamanders. First, parsimony analysis provides no convincing phylogenetic groupings of salamander families other than the Cryptobranchidae and the clade containing all salamanders (Urodela). Likelihood-based estimates of branch lengths show that the branches grouping two or more salamander families are very short relative to those immediately ancestral to individual families. Our simulations show that these conditions are ones in which model-based methods of phylogenetic reconstruction should outperform parsimony analysis.

Model-based methods nonetheless find statistical support for groupings of families that seem anomalous based on prior information (Larson and Dimmick, 1993; Chippindale et al., 2004; Wiens et al., 2005). Specifically, branches A and B on Figure 4b both receive strong support by the model-based analyses, and both require rejection of monophyly of salamander suborder Salamandroidea, which comprises all internally fertilizing salamanders. Both of these branches are recovered independently by model-based analyses of nuclear rRNA gene sequences, although only branch A receives statistical support from these analyses (Fig. 3). Reasons for considering these results anomalous include (1) support for a monophyletic Salamandroidea in parsimony and Bayesian analyses of nuclear RAG-1 sequences combined with the rRNA sequences and other mitochondrial genomic sequences (Chippindale et al., 2004; Wiens et al., 2005), and (2) expected evolutionary stability of the internal-fertilization system as a synapomorphy of Salamandroidea.

The internal-fertilization system of Salamandroidea is a suite of morphological and life-history characteristics considered a functionally burdened complex unlikely to show homoplastic evolution or to be secondarily lost (see discussions by Larson, 1991; Sever and Brizzi, 1998). Male and female cloacal glands associated with internal fertilization are similar among salamandroid families except that spermathecae are more complex structures in plethodontids than in other families (Sever, 1994). Although fertilization is not well documented in Sirenidae, absence of the cloacal glands that function in salamandroid fertilization and absence of sperm in the oviducts of reproductive females strongly suggest external fertilization (Sever et al., 1996) or at least a fertilization system very different from salamandroid fertilization. Internal fertilization appears not to have been lost within any salamandroid families, indicating that it is indispensable to their reproductive biology.

Given strong reasons to expect monophyly of Salamandroidea, the statistical support for branches A and B of Figure 4b from our model-based analyses provides a means to identify conditions under which model-based

methods may produce misleading results. Character support for clades A and B in the maximum-likelihood analyses of mitochondrial DNA data depends largely upon a small number of character positions (Tables 5 and 6) that individually contribute relatively large amounts to total lnL in the maximum-likelihood tree. The high lnL at these positions depends on substitutions expected to be rare for the favored evolutionary model combined with a relatively low evolutionary rate for the character position. The biological interpretation of this result is that homoplasy is unlikely to produce a sharing of derived states for such characters. A major contrast between interpretations of parsimony-based analyses and model-based approaches is that parsimony analysis finds the mitochondrial genomic data equivocal regarding monophyly of Salamandroidea, whereas model-based criteria in the Bayesian analysis reject monophyly of Salamandroidea largely on patterns from heavily weighted characters.

Our results therefore suggest that despite strong evidence for greater statistical power of maximum-likelihood and Bayesian methods relative to unweighted parsimony analysis, the model-based methods may provide misleading results where a parsimony analysis would be more conservative in judging the results inconclusive. Either over- or under simplification of estimated models could produce inaccurate trees with inflated confidence (Buckley, 2002), and model-based phylogenetic methods are not immune to long-branch attraction when evolutionary models are violated (Huelsenbeck, 1997; Swofford et al., 2001).

Statistical support for a mistaken topology is perhaps most likely to occur when resolving relatively short internal branches located deep in the phylogenetic history of a group, especially when some substitutional saturation has occurred in the sequences being compared. In such situations, an analysis of the contributions of individual characters to the statistical significance of model-based results is recommended to determine whether such significance results from a relatively small number of heavily weighted characters, as seen for branches A and B in Figure 4b (Tables 5 and 6). Such outcomes would be most sensitive to errors in estimation of an evolutionary model or temporal changes in an evolutionary model (Lemmon and Moriarty, 2004; Sullivan and Swofford, 1997). This character-based analysis may be the most objective way to identify misleading statistical confidence derived from a Bayesian analysis (Buckley et al., 2001; Buckley, 2002; Goldman et al., 2000).

ACKNOWLEDGEMENTS

This work was supported by the National Science Foundation (DDIG-0105166). We thank M. Fishbein, R. Glor, E. Jockusch, J. Kolbe, K. Kozak, M. Mahoney, K. Nicholson, J. Schulte, T. Townsend, and other members of the Washington University systematics reading group for comments on earlier drafts of this manuscript. We thank Malcolm Tobias for assistance with parallel computing and the Washington University Center for Scientific Parallel Computing for providing computer resources. Jim Wilgenbusch was helpful with PAUP technicalities. Carla Cicero, David Green, Masafumi Matsui, and Paul Moler were kind in providing tissues and museum numbers.

REFERENCES

- Alfaro, M. E., S. Zoller, and F. Lutzeni. 2003. Bayes or bootstrap? A simulation study comparing the performance of Bayesian Markov chain Monte Carlo sampling and bootstrapping in assessing phylogenetic confidence. *Mol. Biol. Evol.* 20:255–266.
- Altekar, G., S. Dwarkadas, J. P. Huelsenbeck, and F. Ronquist. 2004. Parallel Metropolis coupled Markov chain Monte Carlo for Bayesian phylogenetic inference. *Bioinformatics* 20:407–415.
- Anderson, S., A. T. Bankier, B. G. Barrell, M. H. L. de Bruijn, A. R. Coulson, J. Drouin, I. C. Eperon, D. P. Nierlich, B. A. Roe, F. Sanger, P. H. Schreier, A. J. H. Smith, R. Staden, and I. G. Young. 1981. Sequence and organization of the human mitochondrial genome. *Nature* 290: 457–465.
- Bermingham, E., S. S. McCafferty, and A. P. Martin. 1997. Fish biogeography and molecular clocks: Perspectives from the Panamanian Isthmus. Pages 113–128 in *Molecular systematics of fishes* (T. D. Kocher, and C. A. Stepien, eds.). Academic Press, San Diego, California.
- Bremer, K. 1994. Branch support and tree stability. *Cladistics* 10:295–304.
- Buckley, T. R. 2002. Model misspecification and probabilistic tests of topology: Evidence from empirical data sets. *Syst. Biol.* 51:509–523.
- Buckley, T. R., C. Simon, S. Shimodaira, and G. K. Chambers. 2001. Evaluating hypotheses on the origin and evolution of the New Zealand alpine cicadas (*Maoricicada*) using multiple-comparison tests of tree topology. *Mol. Biol. Evol.* 18:223–234.
- Chippindale, P. T., R. M. Bonnet, A. S. Baldwin, and J. J. Wiens. 2004. Phylogenetic evidence for a major reversal of life-history evolution in plethodontid salamanders. *Evolution* 58:2809–2822.
- Donoghue, M. J. 1989. Phylogenies and the analysis of evolutionary sequences, with examples from seed plants. *Evolution* 43:1137–1156.
- Donoghue, M. J., and M. J. Sanderson. 1992. The suitability of molecular and morphological evidence in reconstructing plant phylogeny. Pages 340–368 in *Molecular systematics of plants* (P. S. Soltis, D. E. Soltis, and J. J. Doyle, eds.). Chapman and Hall, New York.
- Duellman, W. E., and L. Trueb. 1986. *Biology of amphibians*. McGraw Hill, New York.
- Felsenstein, J. 1978. Cases in which parsimony or compatibility methods will be positively misleading. *Syst. Zool.* 27:401–410.
- Felsenstein, J. 1985. Confidence limits on phylogenies with a molecular clock. *Syst. Zool.* 34:152–161.
- Fishbein, M., C. Hibsch-Jetter, D. E. Soltis, and L. Hufford. 2001. Phylogeny of Saxifragales (Angiosperms, Eudicots): Analysis of a rapid, ancient radiation. *Syst. Biol.* 50:817–847.
- Gao, K. Q., and N. H. Shubin. 2001. Late Jurassic salamanders from northern China. *Nature* 410:574–577.
- Gao, K. Q., and N. H. Shubin. 2003. Earliest known crown-group salamanders. *Nature* 422:424–428.
- Goldman, N., J. P. Anderson, and A. G. Rodrigo. 2000. Likelihood-based tests of topologies in phylogenetics. *Syst. Biol.* 49:652–670.
- Goldman, N., and S. Whelan. 2000. Statistical tests of gamma-distributed rate heterogeneity in models of sequence evolution in phylogenetics. *Mol. Biol. Evol.* 17:975–978.
- Halanych, K. M. 1998. Considerations for reconstructing metazoan history: Signal, resolution, and hypothesis testing. *Am. Zool.* 38:929–941.
- Halanych, K. M., J. R. Demboski, J. R., B. J. van Vuuren, D. R. Klein, and J. A. Cook. 1999. Cytochrome b phylogeny of North American hares and jackrabbits (*Lepus*, *Lagomorpha*) and the effects of saturation in outgroup taxa. *Mol. Phylogenet. Evol.* 11:213–221.
- Hasegawa, M., H. Kishino, and T. Yano. 1985. Dating of the human-ape splitting by a molecular clock of mitochondrial DNA. *J. Mol. Evol.* 21:160–174.
- Hay, J. M., I. Ruvinsky, S. B. Hedges, and L. R. Maxson. 1995. Phylogenetic relationships of amphibian families inferred from DNA sequences of mitochondrial 12S and 16S ribosomal RNA genes. *Mol. Biol. Evol.* 12:928–937.
- Hillis, D. M. 1996. Inferring complex phylogenies. *Nature* 383:130–131.
- Hillis, D. M., J. P. Huelsenbeck, and C. W. Cunningham. 1994. Application and accuracy of molecular phylogenies. *Science* 264: 671–677.
- Hrbek, T., and A. Larson. 1999. The evolution of diapause in the killifish family Rivulidae (Atherinomorpha, Cyprinodontiformes): A

- molecular phylogenetic and biogeographic perspective. *Evolution* 53:1200–1216.
- Huelsenbeck, J. P. 1995. Performance of phylogenetic methods in simulation. *Syst. Biol.* 44:17–48.
- Huelsenbeck, J. P. 1997. Is the Felsenstein zone a fly trap? *Syst. Biol.* 46:69–74.
- Huelsenbeck, J. P. 1998. Systematic bias in phylogenetic analysis: Is the Strepsiptera problem solved? *Syst. Biol.* 47:519–537.
- Huelsenbeck, J. P., and F. Ronquist. 2001. MRBAYES: Bayesian inference of phylogenetic trees. *Bioinformatics* 17:754–755.
- Huelsenbeck, J. P., F. Ronquist, R. Nielsen, and J. P. Bollback. 2001. Bayesian inference of phylogeny and its impact on evolutionary biology. *Science* 294:2310–2314.
- Jackman, T. R., A. Larson, K. de Queiroz, and J. B. Losos. 1999. Phylogenetic relationships and tempo of early diversification in *Anolis* lizards. *Syst. Biol.* 48:254–285.
- Knowles, L. L. 2000. Tests of Pleistocene speciation in montane grasshoppers (genus *Melanoplus*) from the sky islands of western North America. *Evolution* 54:1337–1348.
- Kumazawa, Y., and M. Nishida. 1993. Sequence evolution of mitochondrial transfer RNA genes and deep-branch animal phylogenetics. *J. Mol. Evol.* 37:380–398.
- Larget, B., and D. L. Simon. 1999. Markov chain Monte Carlo algorithms for the Bayesian analysis of phylogenetic trees. *Mol. Biol. Evol.* 16:750–759.
- Larson, A. 1991. A molecular perspective on the evolutionary relationships of the salamander families. *Evol. Biol.* 25:211–277.
- Larson, A. 1998. The comparison of morphological and molecular data in phylogenetic systematics. Pages 275–296 in *Molecular ecology and evolution: Approaches and applications* (R. DeSalle, and B. Schierwater, eds.). Birkhäuser Verlag, Basel, Switzerland.
- Larson, A., and W. W. Dimmick. 1993. Phylogenetic relationships of the salamander families: An analysis of congruence among morphological and molecular characters. *Herpetol. Monogr.* 7:77–93.
- Larson, A., D. W. Weisrock and K. H. Kozak. 2003. Phylogenetic systematics of salamanders (Amphibia: Urodela), a review. Pages 31–108 in *Reproductive biology and phylogeny of Urodela (Amphibia)* (D. M. Sever (ed.)). Science Publishers, Inc., Enfield, New Hampshire.
- Lemmon, A. R., and E. C. Moriarty. 2004. The importance of proper model assumption in Bayesian phylogenetics. *Syst. Biol.* 53:265–277.
- Lewis, P. O. 2001. A likelihood approach to estimating phylogeny from discrete morphological character data. *Syst. Biol.* 50:913–925.
- Macey, J. R., A. Larson, N. B. Ananjeva, Z. L. Fang, and T. J. Papenfuss. 1997a. Two novel gene orders and the role of light-strand replication in rearrangement of the vertebrate mitochondrial genome. *Mol. Biol. Evol.* 14:91–104.
- Macey, J. R., A. Larson, N. B. Ananjeva, and T. J. Papenfuss. 1997b. Replication slippage may cause parallel evolution in the secondary structures of mitochondrial transfer RNAs. *Mol. Biol. Evol.* 14:30–39.
- Macey, J. R., J. A. Schulte, N. B. Ananjeva, A. Larson, N. Rastegar-Pouyani, S. M. Shammakov, and T. J. Papenfuss. 1998a. Phylogenetic relationships among agamid lizards of the *Laudakia caucasia* species group: Testing hypotheses of biogeographic fragmentation and an area cladogram for the Iranian Plateau. *Mol. Phylogenetic Evol.* 10:118–131.
- Macey, J. R., J. A. Schulte, A. Larson, N. B. Ananjeva, Y. Z. Wang, R. Pethiyagoda, N. Rastegar-Pouyani, and T. J. Papenfuss. 2000. Evaluating trans-Tethys migration: An example using acrodont lizard phylogenetics. *Syst. Biol.* 49:233–256.
- Macey, J. R., J. A. Schulte, A. Larson, Z. L. Fang, Y. Z. Wang, B. S. Tuniyev, and T. J. Papenfuss. 1998b. Phylogenetic relationships of toads in the *Bufo bufo* species group from the eastern escarpment of the Tibetan Plateau: A case of vicariance and dispersal. *Mol. Phylogenetic Evol.* 9:80–87.
- Macey, J. R., J. A. Schulte, A. Larson, B. S. Tuniyev, N. Orlov, and T. J. Papenfuss. 1999. Molecular phylogenetics, tRNA evolution, and historical biogeography in anguid lizards and related taxonomic families. *Mol. Phylogenetic Evol.* 12:250–272.
- Macey, J. R., J. L. Strasburg, J. A. Brisson, V. T. Vredenburg, M. Jennings, and A. Larson. 2001. Molecular phylogenetics of western North American frogs of the *Rana boylii* species group. *Mol. Phylogenetic Evol.* 19:131–143.
- Maddison, W. P. 1989. Reconstructing character evolution on polytymous cladograms. *Cladistics* 5:365–377.
- Maddison, W. P., and D. R. Maddison. 2000. MacClade4: Analysis of phylogeny and character evolution, version 4.0. Sinauer Associates, Sunderland, Massachusetts.
- Misof, B., A. M. Rickert, T. R. Buckley, G. Fleck, and K. P. Sauer. 2001. Phylogenetic signal and its decay in mitochondrial SSU and LSU rRNA gene fragments of Anisoptera. *Mol. Biol. Evol.* 18:27–37.
- Nylander, J. A. A., F. Ronquist, J. P. Huelsenbeck, and J. L. Nieves-Aldrey. 2004. Bayesian phylogenetic analysis of combined data. *Syst. Biol.* 53:47–67.
- Philippe, H., A. Chenuil, and A. Adoutte. 1994. Can the Cambrian explosion be inferred through molecular phylogeny? *Development* (Cambridge) Supplement:15–25.
- Poe, S. 2003. Evaluation of the strategy of long-branch subdivision to improve accuracy of phylogenetic methods. *Syst. Biol.* 52:423–428.
- Poe, S., and A. L. Chubb. 2004. Birds in a bush: Five genes indicate explosive evolution of avian orders. *Syst. Biol.* 53:404–415.
- Poe, S., and D. L. Swofford. 1999. Taxon sampling revisited. *Nature* 398:299–300.
- Posada, D., and K. A. Crandall. 1998. Model Test: Testing the model of DNA substitution. *Bioinformatics* 14:817–818.
- Rambaut, A., and N. C. Grassly. 1997. Seq-Gen: An application for the Monte Carlo simulation of DNA sequence evolution along phylogenetic trees. *Comput. Appl. Biosci.* 13:235–238.
- Riedl, R. 1978. Order in living organisms. Wiley, New York.
- Salim, M., and B. E. H. Maden. 1981. Nucleotide sequence of *Xenopus laevis* 18S ribosomal RNA inferred from the gene sequence. *Nature* 291:205–208.
- Schlüter, D. 2000. The ecology of adaptive radiation. Oxford University Press, Oxford, England.
- Sever, D. M. 1991a. Comparative anatomy and phylogeny of the cloacae of salamanders (Amphibia, Caudata). 1. Evolution at the family level. *Herpetologica* 47:165–193.
- Sever, D. M. 1991b. Comparative anatomy and phylogeny of the cloacae of salamanders (Amphibia, Caudata). 2. Cryptobranchidae, Hynobiidae, and Sirenidae. *J. Morphol.* 207:283–301.
- Sever, D. M. 1994. Observations on regionalization of secretory activity in the spermathecae of salamanders and comments on phylogeny of sperm storage in female amphibians. *Herpetologica* 50:383–397.
- Sever, D. M., and R. Brizzi. 1998. Comparative biology of sperm storage in female salamanders. *J. Exp. Zool.* 282:460–476.
- Sever, D. M., L. C. Rania, and J. D. Krenz. 1996. Reproduction of the salamander *Siren intermedia* Le Conte with special reference to oviductal anatomy and mode of fertilization. *J. Morphol.* 227:335–348.
- Shimodaira, H., and M. Hasegawa. 1999. Multiple comparisons of log-likelihoods with applications to phylogenetic inference. *Mol. Biol. Evol.* 16:1114–1116.
- Simmons, M. P., K. M. Pickett, and M. Miya. 2004. How meaningful are Bayesian support values. *Mol. Biol. Evol.* 21:188–199.
- Slowinski, J. B. 2001. Molecular polytomies. *Mol. Phylogenetic Evol.* 19:114–120.
- Sorenson, M. D. 1999. TreeRot, version 2. Boston University.
- Sullivan, J., and D. L. Swofford. 1997. Are guinea pigs rodents? The utility of models in molecular phylogenetics. *J. Mammal. Evol.* 4:77–86.
- Suzuki, Y., G. V. Glazko, and M. Nei. 2002. Overcredibility of molecular phylogenies obtained by Bayesian phylogenetics. *Proc. Natl. Acad. Sci. USA* 99:16138–16143.
- Swofford, D. L. 2002. PAUP*. Phylogenetic analysis using parsimony (* and other methods), version 4. Sinauer Associates, Sunderland, Massachusetts.
- Swofford, D. L., G. J. Olsen, P. J. Waddell, and D. M. Hillis. 1996. Optimality criteria II: Methods based on models of evolutionary change. Pages 426–503 in *Molecular systematics* (D. M. Hillis, C. Moritz, and B. K. Mable, eds.). Sinauer Associates, Sunderland, Massachusetts.
- Swofford, D. L., P. J. Waddell, J. P. Huelsenbeck, P. G. Foster, P. O. Lewis, and J. S. Rogers. 2001. Bias in phylogenetic estimation and its relevance to the choice between parsimony and likelihood methods. *Syst. Biol.* 50:525–539.
- Templeton, A. R. 1983. Phylogenetic inference from restriction endonuclease cleavage site maps with particular reference to the evolution of humans and the apes. *Evolution* 37:221–244.

- Titus, T. A., and A. Larson. 1995. A molecular phylogenetic perspective on the evolutionary radiation of the salamander family Salamandridae. *Syst. Biol.* 44:125–151.
- Trontelj, P., and S. Goricki. 2003. Monophyly of the family Proteidae (Amphibia: Caudata) tested by phylogenetic analysis of mitochondrial 12S rDNA sequences. *Nat. Croat.* 12:113–120.
- Trueb, L. 1993. Patterns of cranial diversity among the Lissamphibia. Pages 255–343 in *The skull* (J. Hanken, and B. K. Hall, eds.). University of Chicago Press, Chicago, Illinois.
- Waddell, P. J., H. Kishino, and H. Ota. 2001. A phylogenetic foundation for comparative mammalian genomics. *Genome Informatics* 12:141–154.
- Walsh, H. E., M. G. Kidd, T. Moum, and V. L. Friesen. 1999. Polytomies and the power of phylogenetic inference. *Evolution* 53:932–937.
- Weisrock, D. W., J. R. Macey, I. H. Ugurtas, A. Larson, and T. J. Papenfuss. 2001. Molecular phylogenetics and historical biogeography among salamanders of the “true” salamander clade: Rapid branching of numerous highly divergent lineages in *Mertensiella luschani* associated with the rise of Anatolia. *Mol. Phylogenet. Evol.* 18:434–448.
- Wiens, J. J. 2003. Missing data, incomplete taxa, and phylogenetic accuracy. *Syst. Biol.* 52:528–538.
- Wiens, J. J., R. M. Bonett, and P. T. Chippindale. 2005. Ontogeny discombobulates phylogeny: Paedomorphosis and higher-level salamander relationships. *Syst. Biol.* 54:91–110.
- Wilcox, T. P., D. J. Zwickl, T. A. Heath, and D. M. Hillis. 2002. Phylogenetic relationships of the dwarf boas and a comparison of Bayesian and bootstrap measures of phylogenetic support. *Mol. Phylogenet. Evol.* 25:361–371.
- Yang, Z. H. 1994. Maximum likelihood phylogenetic estimation from DNA sequences with variable rates over sites: Approximate methods. *J. Mol. Evol.* 39:306–314.
- Yang, Z. H., and B. Rannala. 1997. Bayesian phylogenetic inference using DNA sequences: A Markov Chain Monte Carlo method. *Mol. Biol. Evol.* 14:717–724.

*First submitted 23 June 2004; reviews returned 16 November 2004;
final acceptance 25 March 2005*

Associate Editor: Elizabeth Jockusch



Terrestrial stages of eastern North American salamanders *Desmognathus ochrophaeus* (Plethodontidae, top) and *Notophthalmus viridescens* (Salamandridae, bottom). Photos by David Weisrock.